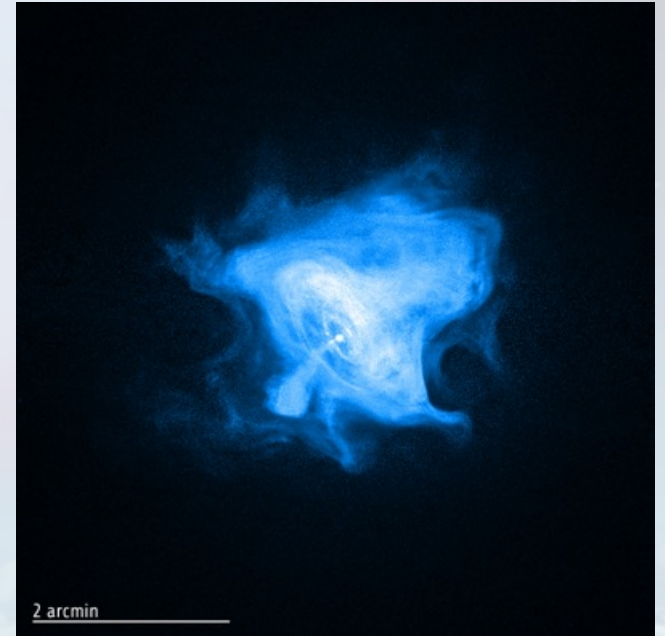


High Energy Particle Astrophysics

Charles Timmermans

Focus of my lectures:

- Detection of:
 - Cosmic Rays
 - TeV gamma's
 - Neutrino's
- Status and results of:
 - Cosmic Ray Physics
 - Neutrino telescopes
 - Air cherenkov gamma detectors



Contents of the Lectures

- Lecture 1+2: Air Showers and Detectors
 - Thomas K. Gaisser, Cosmic Rays and Particle Physics, Cambridge University Press, 1990
 - Detection and interaction of particles
- Lectures 3+4: Results in High Energy Astroparticle physics
 - Cosmic Ray air shower detectors, neutrino telescopes and TeV gamma detectors



Air Showers

Thomas K. Gaisser, Cosmic Rays and Particle Physics, Cambridge University Press, 1990

+ Slides from Ralph Engel (Karlsruhe)

(Detection of) Air Showers

- Charged Cosmic Rays, photons and neutrinos have standard interactions with matter, which creates air showers (or allow detection)

EM Processes in Matter

Coulomb Scattering
Ionization Loss
Cherenkov Effect
Compton Scattering
Bremsstrahlung
Pair creation

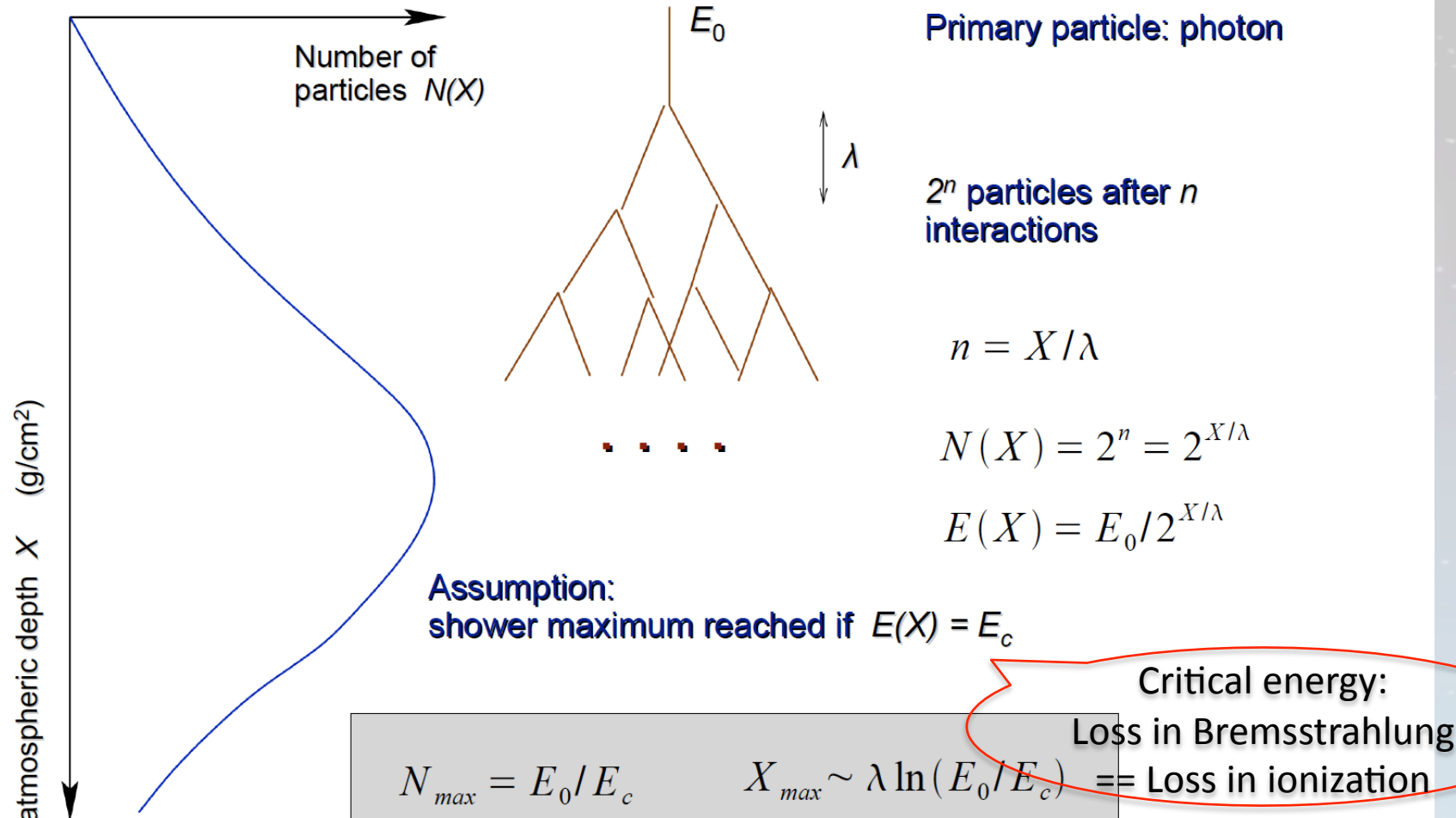
EM Processes on B/photon fields

Synchrotron Radiation
Inverse Compton effect

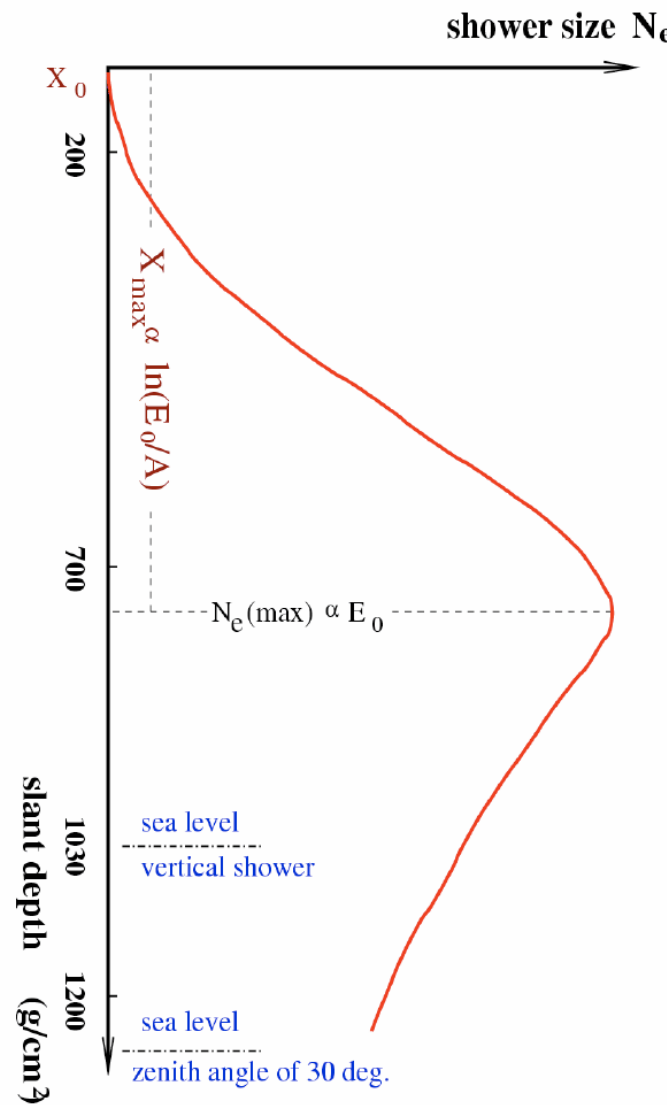
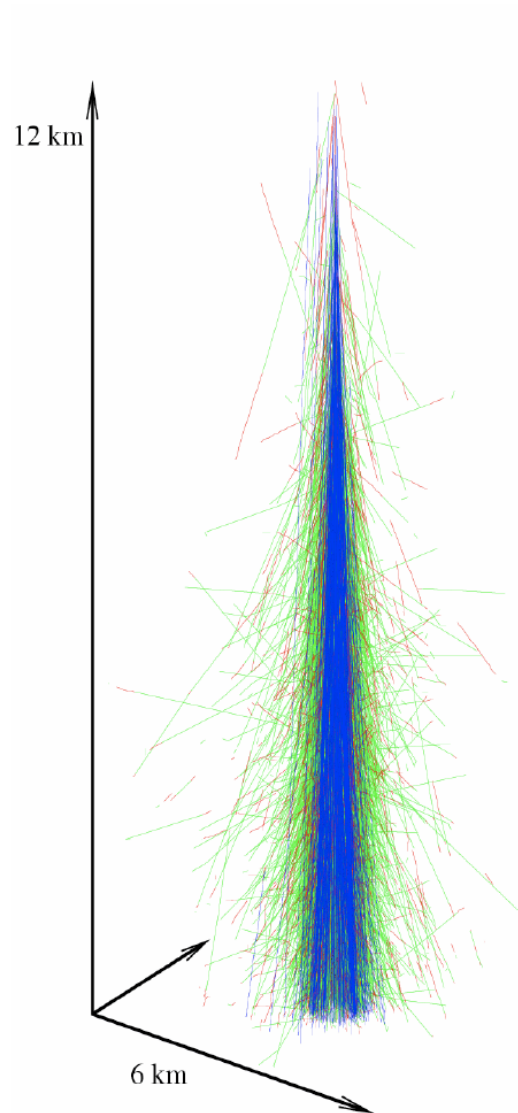
Example: Photon on atmosphere

- A High energy photon in the atmosphere will:
 - Produce e^+e^- pairs influenced by nuclear fields
 - Electron/positron will undergo Bremsstrahlung, resulting in electron/positron and high energy photon
- This sequence of processes continues until critical energy and creates EM cascade

Heitlers Model of EM shower



Characterization of extensive air showers



Atmospheric depth:

$$\int_h^{\infty} \rho(l) dl = X(h)$$

- Shower particles: mainly e^{\pm}, γ
- 80 – 95% of primary energy converted to ionization energy
- Up to 10^{11} charged particles

Process Detail: Bremsstrahlung

$$\frac{dE}{dx} = -\frac{N_A}{A} \int_0^{E-mc^2} \sigma_{br}(E, k) k dk$$

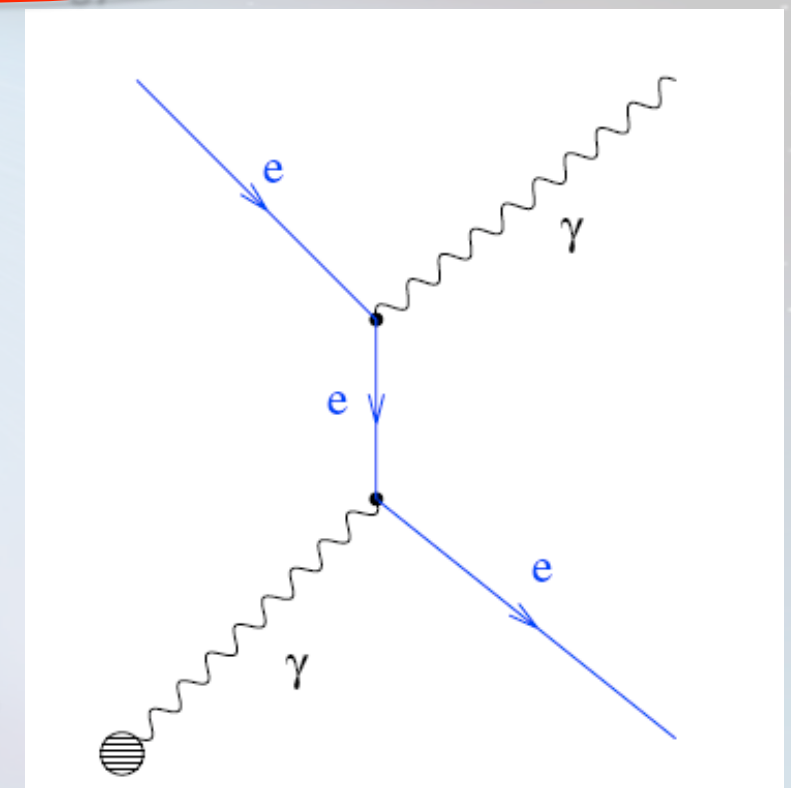
Integrate over emitted photon energy

Number of nuclei encountered

After integration (no screening!)

$$\frac{dE}{dx} = \frac{4N_A Z(Z+1)}{A} ar_e^2 E \left[\ln 191 Z^{-\frac{1}{3}} \right]$$

Interaction with electron field



Introduction of radiation length: $X_0 = \left[\frac{4N_A}{A} Z(Z+1) ar_e^2 \ln(191 Z^{-\frac{1}{3}}) \right]^{-1}$

$$X_0(O_2) = 34.24 \text{ g/cm}^2 \quad X_0(N_2) = 37.99 \text{ g/cm}^2$$

7 Sept 2010

C Timmermans, Ravelli, RND

Process Detail: Pair Creation

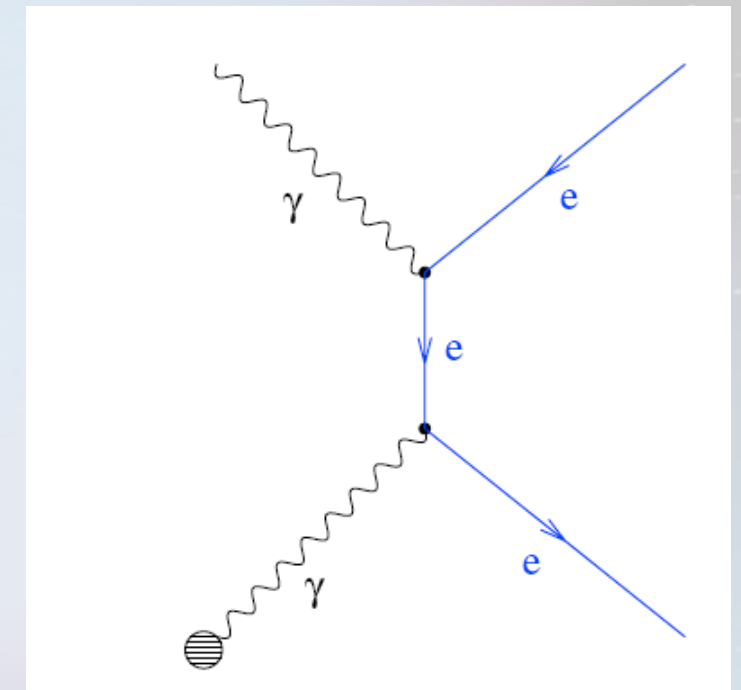
- Inverse process wrt Bremsstrahlung

$$\sigma_{pair}(k, E) = \sigma_{br}(E, k) \cdot \frac{E^2}{k^2} = \frac{4Z^2 ar_e^2}{k} G(k, E)$$

$G(k, E)$ is of order 1

In the case of no screening:

$$\sigma_{pair} = \frac{4}{9} Z^2 ar_e^2 \ln\left(191 Z^{-\frac{1}{3}}\right) - \frac{1}{54}$$



Pair production of
electron field

Bethe-Bloch Formula

Ionization

[see e.g. PDG 2010]

$$-\left\langle \frac{dE}{dx} \right\rangle = K z^2 \frac{Z}{A} \frac{1}{\beta^2} \left[\frac{1}{2} \ln \frac{2m_e c^2 \beta^2 \gamma^2 T_{\max}}{I^2} - \beta^2 - \frac{\delta(\beta\gamma)}{2} \right]$$

[$\cdot \rho$]

density

$$K = 4\pi N_A r_e^2 m_e c^2 = 0.307 \text{ MeV g}^{-1} \text{ cm}^2$$

$$N_A = 6.022 \cdot 10^{23}$$

[Avogardo's number]

$$T_{\max} = 2m_e c^2 \beta^2 \gamma^2 / (1 + 2\gamma m_e/M + (m_e/M)^2)$$

[Max. energy transfer in single collision]

$$r_e = e^2 / 4\pi \epsilon_0 m_e c^2 = 2.8 \text{ fm}$$

[Classical electron radius]

z : Charge of incident particle

$$m_e = 511 \text{ keV}$$

[Electron mass]

M : Mass of incident particle

$$\beta = v/c$$

[Velocity]

Z : Charge number of medium

$$\gamma = (1 - \beta^2)^{-1/2}$$

A : Atomic mass of medium

[Lorentz factor]

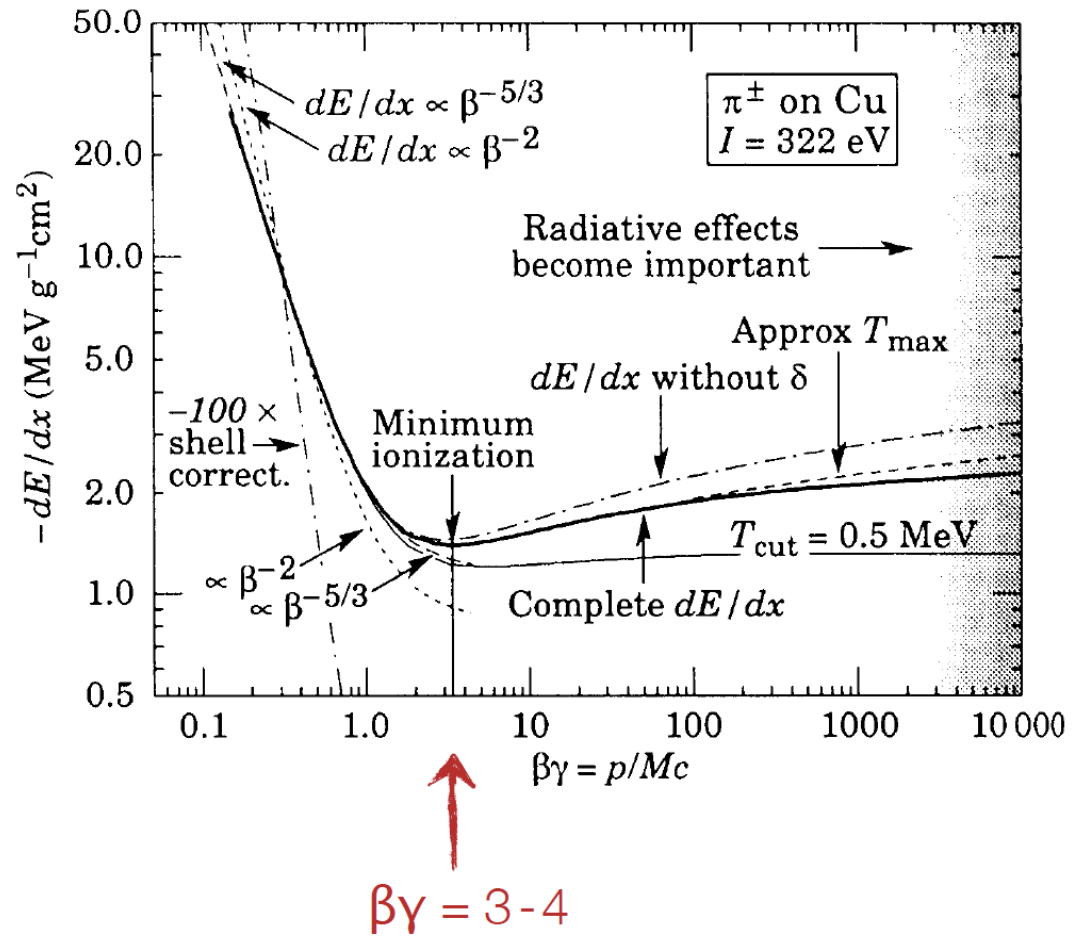
I : Mean excitation energy of medium

Validity:

δ : Density correction [transv. extension of electric field]

$$.05 < \beta\gamma < 500$$
$$M > m_\mu$$

Energy Loss of Pions in Cu



Minimum ionizing particles (MIP): $\beta\gamma = 3-4$

dE/dx falls $\sim \beta^{-2}$; kinematic factor
[precise dependence: $\sim \beta^{-5/3}$]

dE/dx rises $\sim \ln(\beta\gamma)^2$; relativistic rise
[rel. extension of transversal E-field]

Saturation at large ($\beta\gamma$) due to
density effect (correction δ)
[polarization of medium]

Units: $\text{MeV g}^{-1} \text{cm}^2$

MIP losses $\sim 13 \text{ MeV/cm}$
[density of copper: 8.94 g/cm^3]

Understanding Bethe-Bloch

1/ β^2 -dependence:

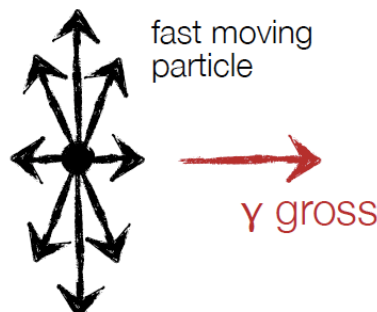
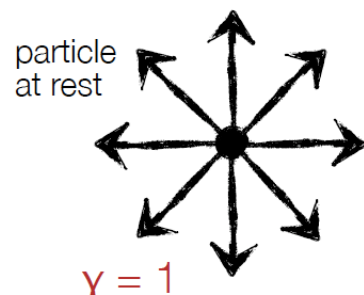
Remember:

$$\Delta p_{\perp} = \int F_{\perp} dt = \int F_{\perp} \frac{dx}{v}$$

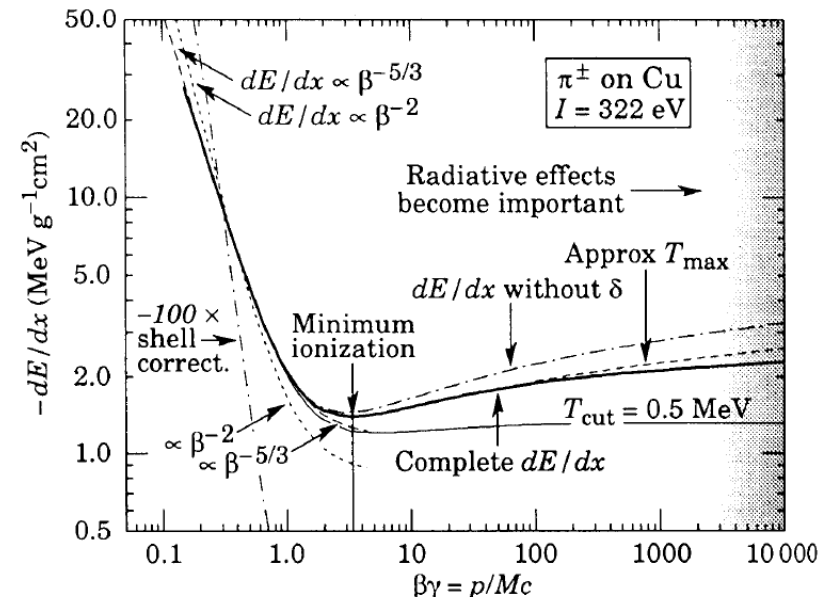
i.e. slower particles feel electric force of atomic electron for longer time ...

Relativistic rise for $\beta\gamma > 4$:

High energy particle: transversal electric field increases due to Lorentz transform; $E_y \rightarrow \gamma E_y$. Thus interaction cross section increases ...



7 sept. 2010



Corrections:

- low energy : shell corrections
- high energy : density corrections

C. Timmermans, Ravelingen BND

Understanding Bethe-Bloch

Density correction:

Polarization effect ...
[density dependent]

→ Shielding of electrical field far from particle path; effectively cuts off the long range contribution ...

More relevant at high γ ...
[Increased range of electric field; larger b_{\max} ; ...]

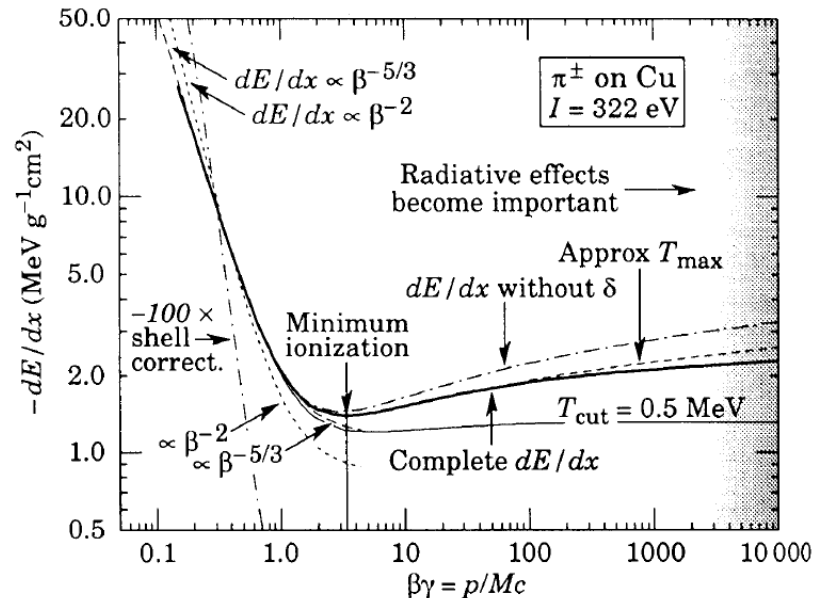
For high energies:

$$\delta/2 \rightarrow \ln(\hbar\omega/I) + \ln\beta\gamma - 1/2$$

Shell correction:

Arises if particle velocity is close to orbital velocity of electrons, i.e. $\beta c \sim v_e$.

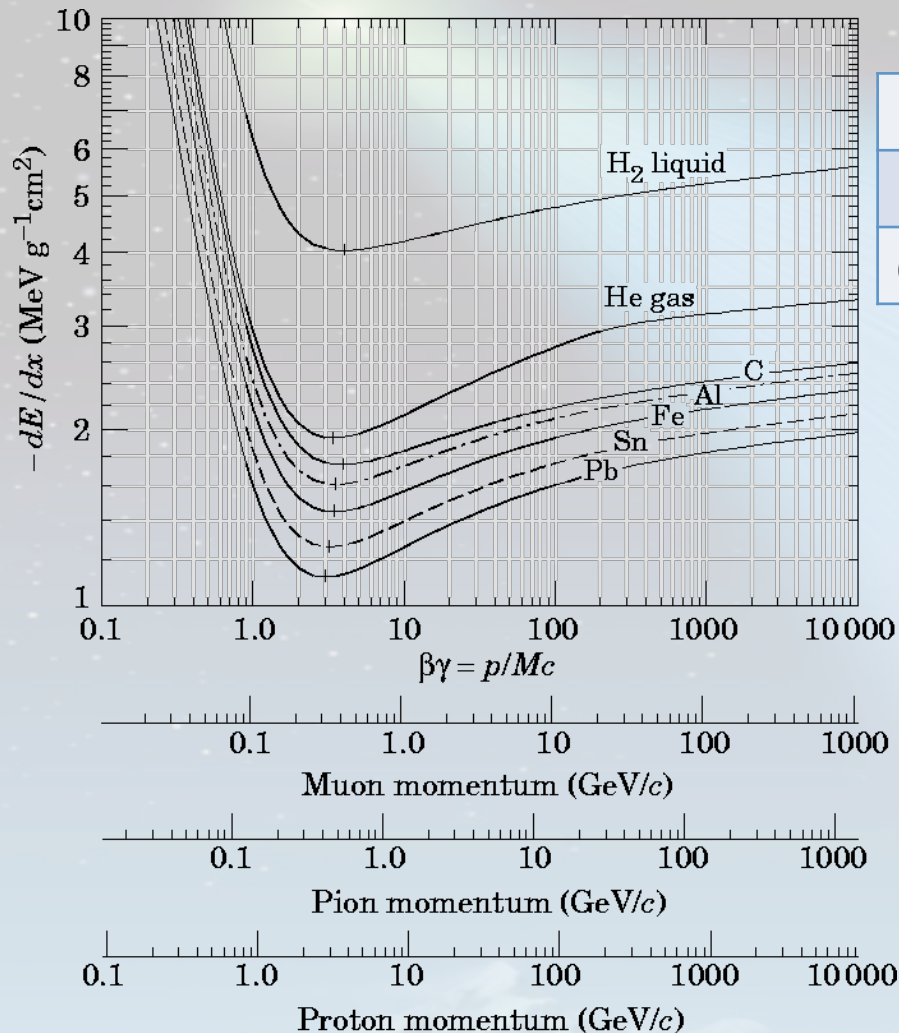
Assumption that electron is at rest breaks down ...
Capture process is possible ...



Density effect leads to saturation at high energy ...

Shell correction are in general small ...

Ionization Loss



Hydrogen	21.8	Nitrogen	90.9
Helium	44.0	Oxygen	104
Carbon	77.8	Iron	286

$$\frac{dE}{dx} = - \frac{N_A Z}{A} \frac{2\pi(z e^2)^2}{M v^2} \left[\ln \frac{2 M v^2 \gamma^2 W}{I^2} - 2 \beta^2 \right]$$

Critical energy

Critical energy:

$$\left. \frac{dE}{dx}(E_c) \right|_{\text{Brems}} = \left. \frac{dE}{dx}(E_c) \right|_{\text{Ion}}$$

Approximation:

$$E_c^{\text{Gas}} = \frac{710 \text{ MeV}}{Z + 0.92}$$

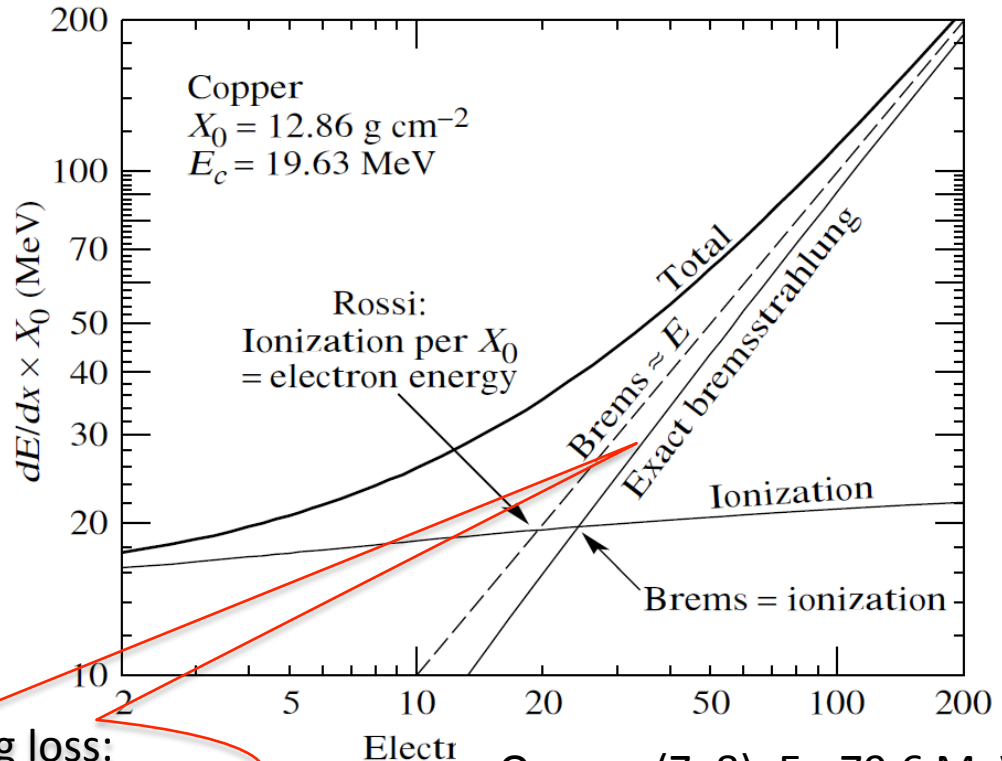
$$E_c^{\text{Sol/Liq}} = \frac{610 \text{ MeV}}{Z + 1.24}$$

Example Copper:

$$E_c \approx 610/30 \approx 20$$

Bremsstrahlung loss:
linear with energy

$$\left(\frac{dE}{dx} \right)_{\text{Tot}} = \left(\frac{dE}{dx} \right)_{\text{Ion}} + \left(\frac{dE}{dx} \right)_{\text{Brems}}$$



And now for real: a photon shower

- Critical energy ~ 80 MeV

Cascade equations (Rossi & Greisen Rev.Mod.Phys. 13, 1940)

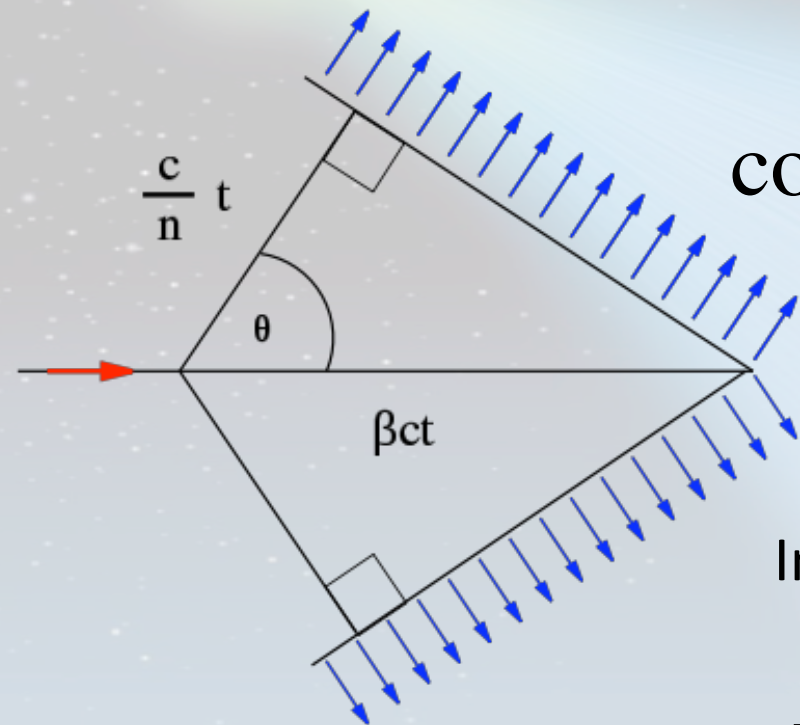
$$\frac{d\phi_e(E)}{dX} = -\frac{1}{\lambda_{\text{brems}}}\phi_e(E) + \int_E^{E_0} \frac{1}{\lambda_{\text{brems}}} \phi_e(\tilde{E}) \frac{dn_{e \rightarrow e}}{dE} d\tilde{E}$$
$$+ \int_E^{E_0} \frac{1}{\lambda_{\text{pair}}} \phi_\gamma(\tilde{E}) \frac{dn_{\gamma \rightarrow e}}{dE} d\tilde{E} + \alpha \frac{\partial \phi_e(E)}{\partial E}$$

Electron flux

Ionization

- In addition: Charged particles go faster than speed of light in atmosphere: Cherenkov effect.

Cherenkov Radiation



$$\cos(\theta) = \frac{1}{\beta n} + q$$

q : small quantum correction

Intensity radiation per unit length:

$$\frac{dN}{dL} = z^2 \frac{\alpha}{\hbar c} \left[1 - \frac{1}{\beta^2 n^2} \right]$$

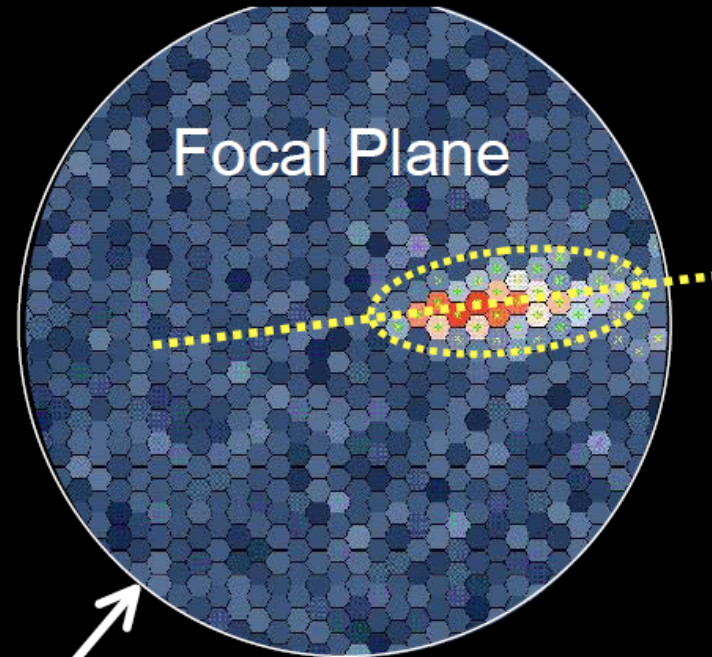
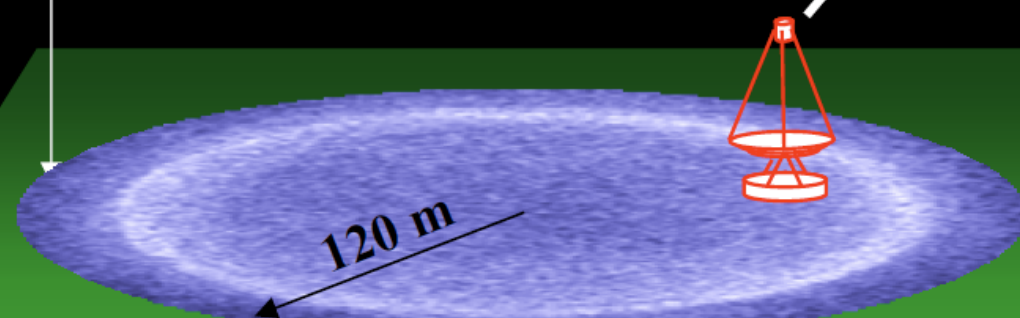
$\frac{\alpha}{\hbar c}$ is about $370 \text{ eV}^{-1} \text{ cm}^{-1}$

Imaging air cherenkov technique (IACT)



7 sept. 2010

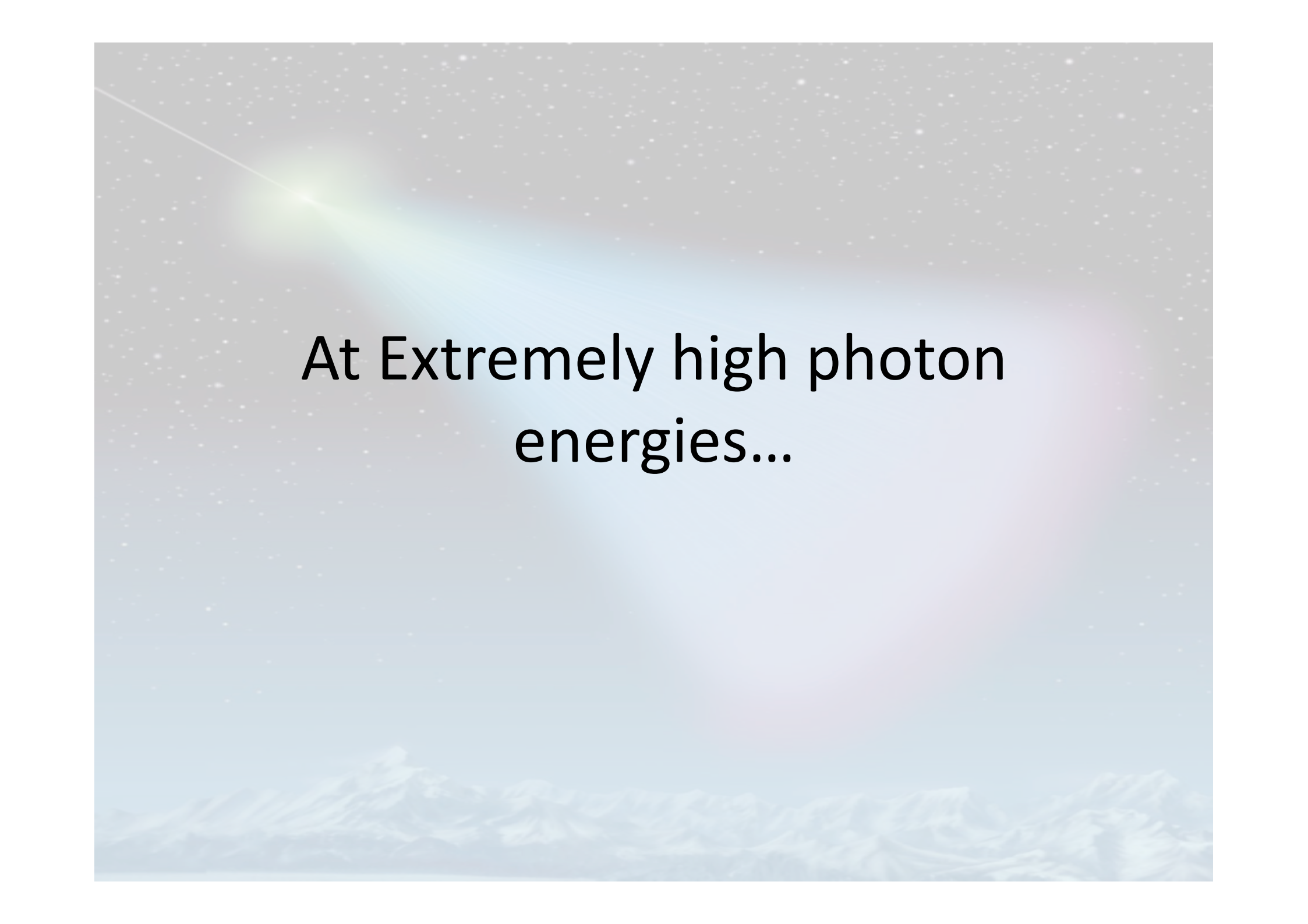
C. Timmermans, Ravelingen BND



Intensity
→ Shower Energy

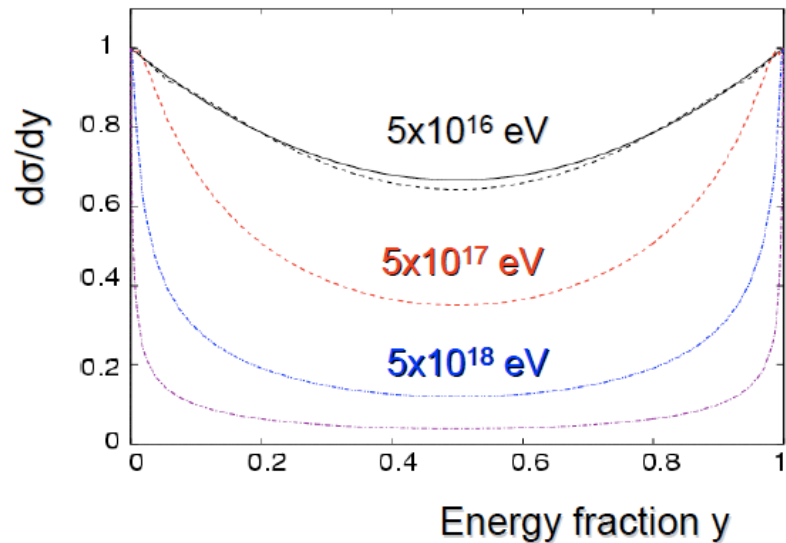
Image Orientation
→ Shower Direction

Image Shape
→ Primary Particle



At Extremely high photon
energies...

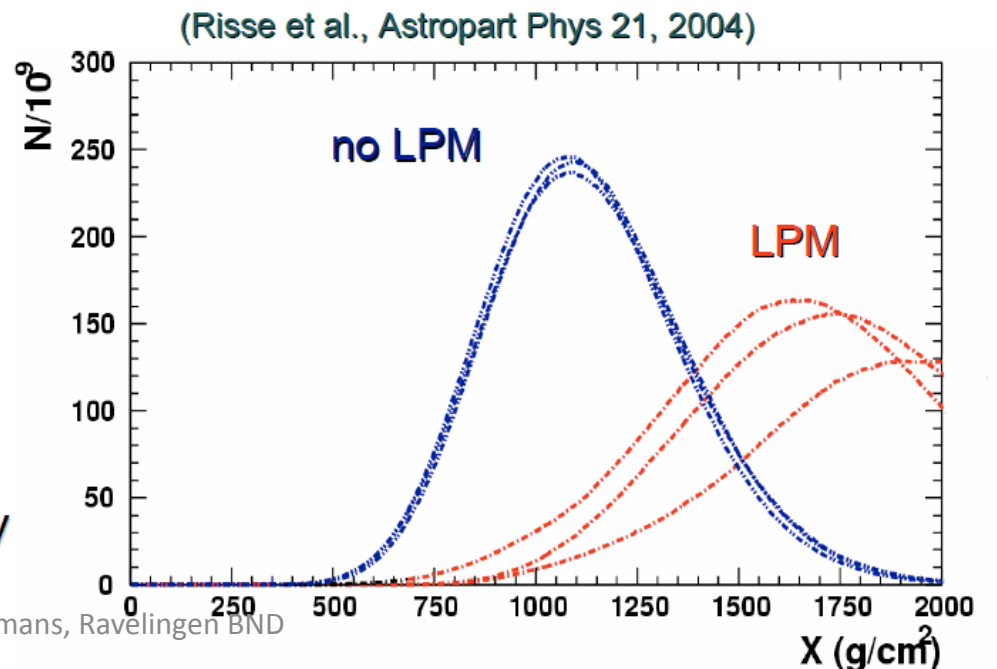
Landau-Pomeranchuk-Migdal effect



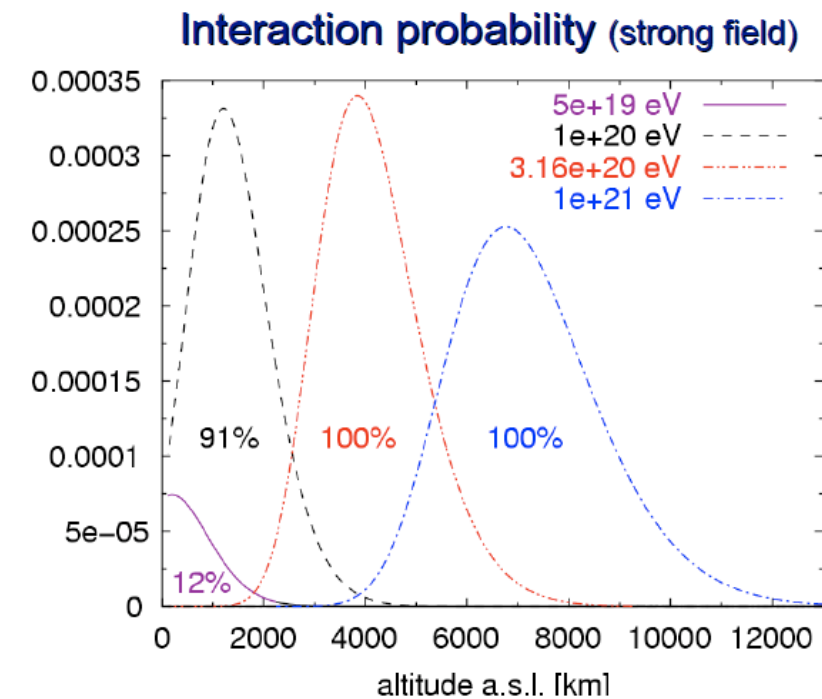
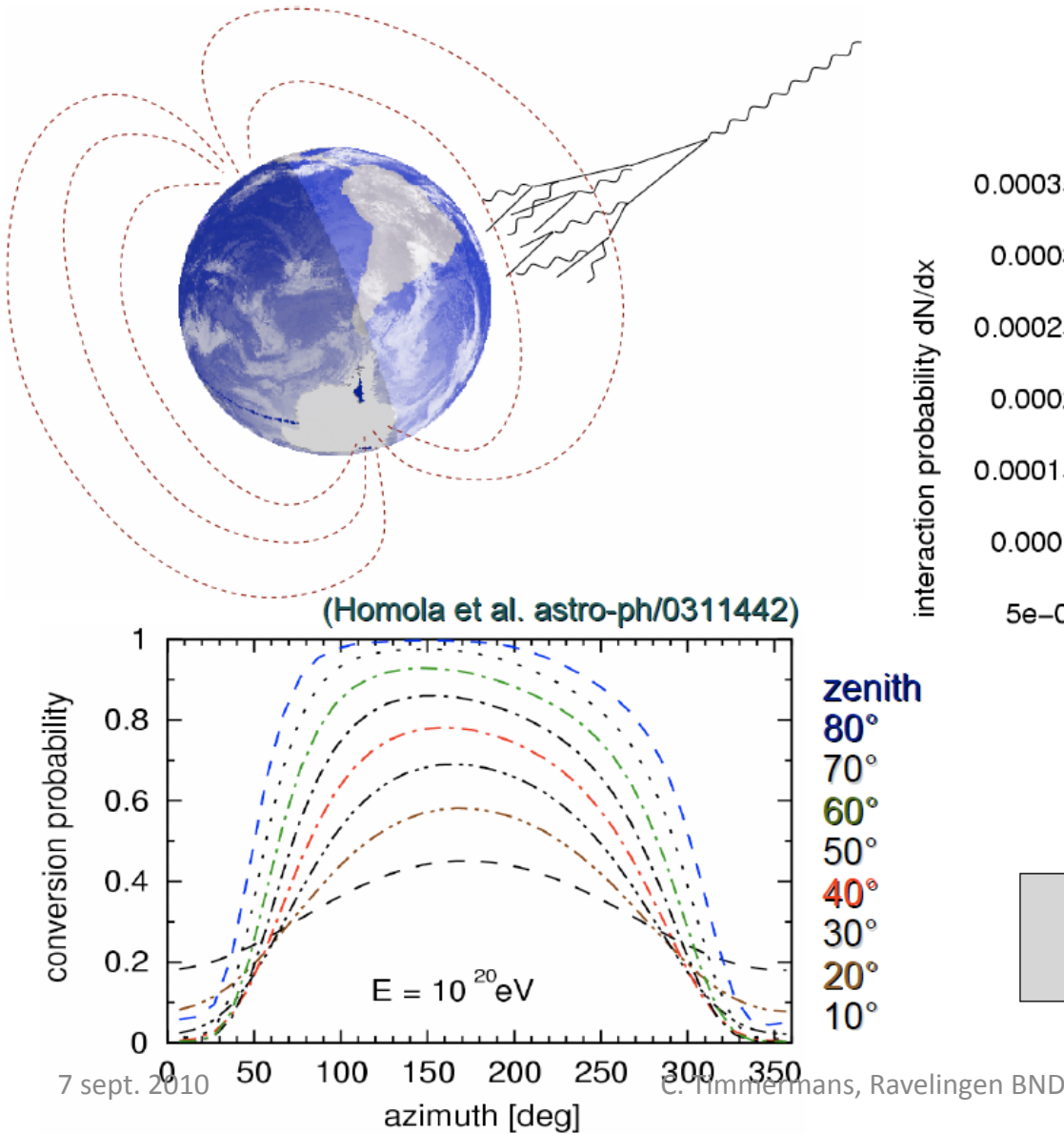
$$S_{\text{supp}} \sim \sqrt{\frac{E_{\text{LPM}}}{y(1-y)E}}$$

Example: photon 3×10^{20} eV

Pair production
(sea level, $E_{\text{LPM}} \sim 10^{17}$ eV)



Pre-showering in geomag. field



Unique signature of photons



Hadrons in the Atmosphere

Nucleon Transport Equations

$$\frac{dN(E, X)}{dX} = -\frac{N(E, X)}{\lambda_N(E)} + \int_E^\infty \frac{N(E', X)}{\lambda_N(E')} F_{NN}(E, E') \frac{dE'}{E}$$

Change in rate of nucleons of energy E rate as function of slant depth

Nucleons of energy E which interact

Nucleons of energy E' which interact and create nucleons of energy E

$$X_v = \int_h^\infty \rho(h') dh'.$$

Density of air at altitude h'

Interaction Length

The probability that a nucleon of energy E interacts is given by:

$$dX/\lambda_N(E)$$

In this equation λ_N is given in gram per cm². Thus this is a probability as function of the amount of air that was seen by the nucleon.

$$\lambda_N = \frac{\rho}{\rho_N \sigma_N^{air}} = \frac{A m_p}{\sigma_N^{air}}$$

300 mb Density of the atmosphere

Number density of nuclei in the atmosphere

$$F_{NN}(E, E')$$

$$F_{ac}(E_c, E_a) = E_c \frac{dn_c(E_c, E_a)}{dE_c}$$

The number of particles (of type c) of energy E_c produced when an incident particle a interacts with the atmosphere:

A dimensionless inclusive cross section

Boundary Condition

The boundary condition now describes the physics of interest:

- 1) A single particle of energy E_0 at the top of the atmosphere: $N(E,0) = A\delta(E-E_0/A)$. One gets the nucleon creation of a single cascade
- 2) A nucleon flux on top of the atmosphere
 $N(E,0) = n_0 E^{-(\gamma+1)}$ nucleons/(cm² sr s GeV/A) .
One gets the flux of nucleons in our atmosphere when using
 $\gamma=1.7$ and $n_0 = 1.8$

Here the latter is evaluated.

Assumptions: Factorization

$$N(E, X) = G(E)g(X)$$

The transport equation then becomes:

$$G \frac{dg}{dX} = -\frac{Gg}{\lambda_N} + g \int_0^1 \frac{G(E/x_L) F_{NN}(x_L, E)}{\lambda_N(E/x_L)} \frac{dx_L}{x_L^2}$$

Where $x_l = E/E'$

Now define:

$$\frac{1}{\Lambda} = \frac{1}{\lambda_N(E)} - \frac{1}{G(E)} \int_0^1 \frac{G(E/x_L) F_{NN}(x_L, E)}{\lambda_N(E/x_L)} \frac{dx_L}{x_L^2}$$

Then:

$$g(X) = g(0) \exp(-X/\Lambda)$$

In this equation Λ is a function of energy !

Assumptions: Approximation A

Approximation A is well known in electromagnetic cascade theory and states:

- 1) Energy loss by ionization can be neglected
- 2) Radiation length is independent of energy
- 3) Cross sections for pair production and bremsstrahlung scale

In our case this means:

$$\lambda_N(E) \sim \lambda_N = \text{constant}$$

$$F_{NN}(x_L, E) \sim F_{NN}(x_L)$$

In reality there is a logarithmic behaviour on the energy!

Solution nucleon transport equations

After factorization we had:

$$g(X) = g(0) \exp(-X/\Lambda)$$

Approximation A makes Λ independent of energy and we get

$$N(E, X) = g(0) \exp(-X/\Lambda) E^{-(\gamma+1)}$$

Spectrum weighted moments

Note that:

$$\frac{1}{\Lambda} = \frac{1}{\lambda_N} \left[1 - \int_0^1 x_L^{\gamma-1} F_{NN}(x_L) dx_L \right]$$

We now define the spectrum weighted moments:

$$Z_{ac} = \int_0^1 x_L^{\gamma-1} F_{ac}(x_L) dx_L$$

This tells which part of the cross section is important. When there is a steeply falling spectrum, only x of about 1 is important, which is the forward part of the cross section.

Coupled Cascade Equations

In reality, from an interaction different types of particles are created. In a next interaction these particles may then create the same type of particles, etc. Thus all interactions in a cascade are coupled:

$$\frac{dN_i(E, X)}{dX} = -N_i(E, X) \left(\frac{1}{\lambda_i} + \frac{1}{d_i} \right) + \sum_j \int_E^\infty \frac{N_j(E_j)}{\lambda_j} \frac{F_{ji}(E_i, E_j)}{E_i} dE_j$$

Particles can decay!

Sum over all possible parents

Lets look at pions

Assumption: pions are created from nucleon and pion to air interactions

$$\begin{aligned}\frac{d\Pi}{dX} = -\Pi \left(\frac{1}{\lambda_\pi} + \frac{1}{d_\pi} \right) + \int_0^1 \frac{\Pi(E/x_L)}{\lambda_\pi(E/x_L)} F_{\pi\pi}(E_\pi, E_\pi/x_L) \frac{dx_L}{x_L^2} \\ + \int_0^1 \frac{N(E/x_L)}{\lambda_N(E/x_L)} F_{N\pi}(E_\pi, E_\pi/x_L) \frac{dx_L}{x_L^2}\end{aligned}$$

New: A loss due to decay

$$\Delta\Pi = -\Pi \frac{\Delta l}{\gamma c \tau_\pi} = -\Pi \frac{\Delta X}{\rho \gamma c \tau_\pi} = -\frac{\Pi}{d_\pi} \Delta X$$

In these units: the decay length depends on the local density of air

Altitude and depth

Different conversions exist, an example is given in the following parameterization

$$h_v(\text{km}) = \begin{cases} 47.05 + 6.9 \ln X_v + 0.299 \ln^2 \left(\frac{X_v}{10} \right) & X_v < 25 \text{g/cm}^2 \\ 45.5 - 6.34 \ln X_v & 25 < X_v < 230 \\ 44.34 - 11.861(X_v)^{0.19} & X_v > 230 \text{g/cm}^2 \end{cases}$$

This should be integrated along the path of the particle to give:

$$\rho = X_v / h_0 = X \cos(\theta) / h_0$$

Evaluated at the appropriate atmospheric depth

Decay vs Interaction

$$\frac{1}{d_\pi} = \frac{1}{\rho \gamma c \tau_\pi} = \frac{m_\pi c^2 h_0}{E c \tau_\pi X \cos \theta} = \frac{\epsilon_\pi}{E X \cos \theta}$$

At an altitude of 6.4 km, one gets $\epsilon_\pi = 115 \text{ GeV}$

When the energy is above 115 GeV, interactions dominate. Below 115 GeV decay should be taken into account

Pions in the atmosphere

Using the nucleon solution one gets:

$$\begin{aligned}\frac{d\Pi}{dX} = & -\Pi(E, X) \left(\frac{1}{\lambda_\pi} + \frac{\epsilon_\pi}{EX \cos \theta} \right) \\ & + \frac{1}{\lambda_\pi} \int_0^1 \Pi(E/x_L, X) F_{\pi\pi}(x_L) \frac{dx_L}{x_L^2} \\ & + \frac{Z_{N\pi}}{\lambda_N} N(E, 0) e^{-X/\Lambda_N}\end{aligned}$$

Again, assuming factorization one obtains an energy dependence as $E^{-(\gamma+1)}$ and

$$\frac{d\Pi}{dX} = -\Pi(E, X) \left(\frac{1}{\Lambda_\pi} + \frac{\epsilon_\pi}{EX \cos \theta} \right) + \frac{Z_{N\pi}}{\lambda_N} N(E, 0) e^{-X/\Lambda_N}$$

Next use the boundary condition that there are no pions on top of the atmosphere. This then gives:

$$\Pi(E, X) = e^{-(X/\Lambda_\pi)} \frac{Z_{N\pi}}{\lambda_N} N_0(E) \int_0^X \left(\frac{X'}{X}\right)^{\epsilon_\pi/E \cos \theta} \exp\left(\frac{X'}{\Lambda_\pi} - \frac{X'}{\Lambda_N}\right) dX'$$

For high energies, pion decay is not important:

$$\Pi(E, X) = N_0(E) \frac{Z_{N\pi}}{1 - Z_{NN}} \frac{\Lambda_\pi}{\Lambda_\pi - \Lambda_N} \left(e^{-X/\Lambda_\pi} - e^{-X/\Lambda_N} \right)$$

For low energies, only X' close to X matters and:

$$\Pi(E, X) = \frac{Z_{N\pi}}{\lambda_N} N_0(E) e^{-X/\Lambda_N} \frac{XE \cos \theta}{\epsilon_\pi}$$

The electromagnetic shower

From the previous, it is clear that the electromagnetic shower is fed from π^0 decay into two photons. The lifetime is 10^{-16} s, thus

$$\epsilon_{\pi^0} = 5.5 \times 10^{10} \text{ GeV}$$

The π^0 decay spectrum thus equals its production spectrum, or

$$\mathcal{D}_{\pi^0} = \frac{N(E, X)}{\lambda_N} Z_{N\pi^0} + \frac{\Pi(E, X)}{\lambda_\pi} Z_{\pi\pi^0} + \dots$$

From the kinematics of a 2 body decay: $\frac{dn_\gamma}{dE_\gamma} = 2/E_{\pi^0}$
Knowing fluxes behave like $E^{-(\gamma+1)}$ one gets:

$$\frac{dn_\gamma(E, X)}{dX} = \frac{2}{\gamma+1} \left(\frac{N(E, X)}{\lambda_N} Z_{N\pi^0} + \frac{\Pi(E, X)}{\lambda_\pi} Z_{\pi\pi^0} \right)$$

Muon Flux

Muon production originates from the decay of kaons and charged pions

$$\begin{aligned}\mathcal{P}_\mu(E, X) = & \frac{\epsilon_\pi}{X \cos \theta(1 - r_\pi)} \int_{E_\mu}^{E_\mu/r_\pi} \frac{\Pi(E, X)}{E} \frac{dE}{E} \\ & + \frac{0.635\epsilon_K}{X \cos \theta(1 - r_K)} \int_{E_\mu}^{E_\mu/r_K} \frac{K(E, X)}{E} \frac{dE}{E}\end{aligned}$$

Neglecting muon decay one gets:

$$\mu(E_\mu, X) = \int_0^X \mathcal{P}_\mu(E, X') dX'$$

Approximate Solution

$$\frac{dN_\mu}{dE_\mu} \simeq \frac{N_0(E_\mu)}{1 - Z_{NN}} \\ \left\{ \mathcal{A}_{\pi\mu} \frac{1}{1 + \mathcal{B}_{\pi\mu} \cos \theta E_\mu / \epsilon_\pi} \right. \\ \left. + 0.635 \mathcal{A}_{K\mu} \frac{1}{1 + \mathcal{B}_{K\mu} \cos \theta E_\mu / \epsilon_K} \right\}$$

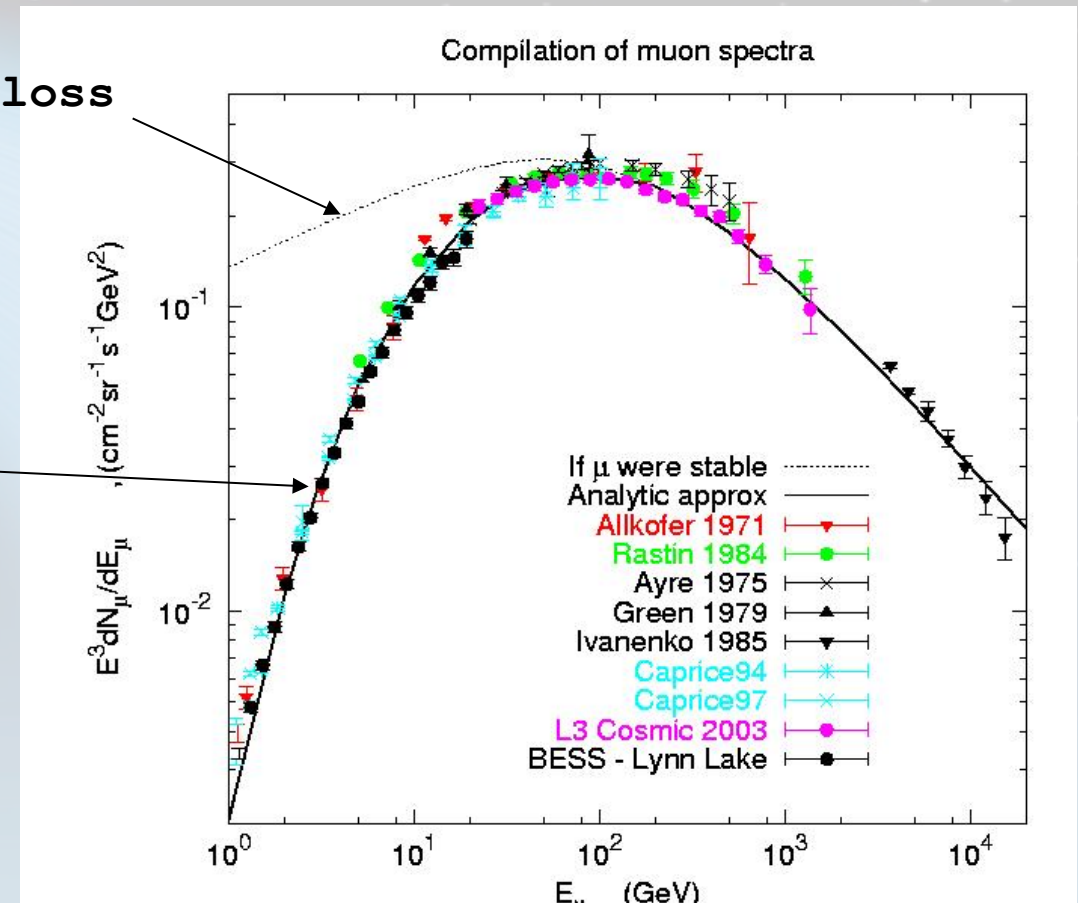
$$\begin{aligned} \mathcal{A}_{\pi\mu} &= Z_{N\pi} \frac{1 - (r_\pi)^{\gamma+1}}{(1 - r_\pi)(\gamma + 1)} \\ \mathcal{B}_{\pi\mu} &= \frac{\gamma + 2}{\gamma + 1} \frac{1 - (r_\pi)^{\gamma+1}}{1 - (r_\pi)^{\gamma+2}} \frac{\Lambda_\pi - \Lambda_N}{\Lambda_\pi \ln(\Lambda_\pi/\Lambda_N)} \end{aligned}$$

$$\frac{dN_\mu}{dE_\mu} \simeq \frac{0.14 E^{-2.7}}{\text{cm}^2 \text{s sr GeV}} \left\{ \frac{1}{1 + \frac{1.1 E_\mu \cos \theta}{115 \text{ GeV}}} + \frac{0.054}{1 + \frac{1.1 E_\mu \cos \theta}{850 \text{ GeV}}} \right\}$$

Account for μ energy loss

Account for μ decay

Analytic approximation
works well!



Muon Charge Ratio

The muon charge ratio is:

$$K_\mu = \frac{\mu^+}{\mu^-} = \frac{1 + \delta_0 \mathcal{A} \mathcal{B}}{1 - \delta_0 \mathcal{A} \mathcal{B}}$$

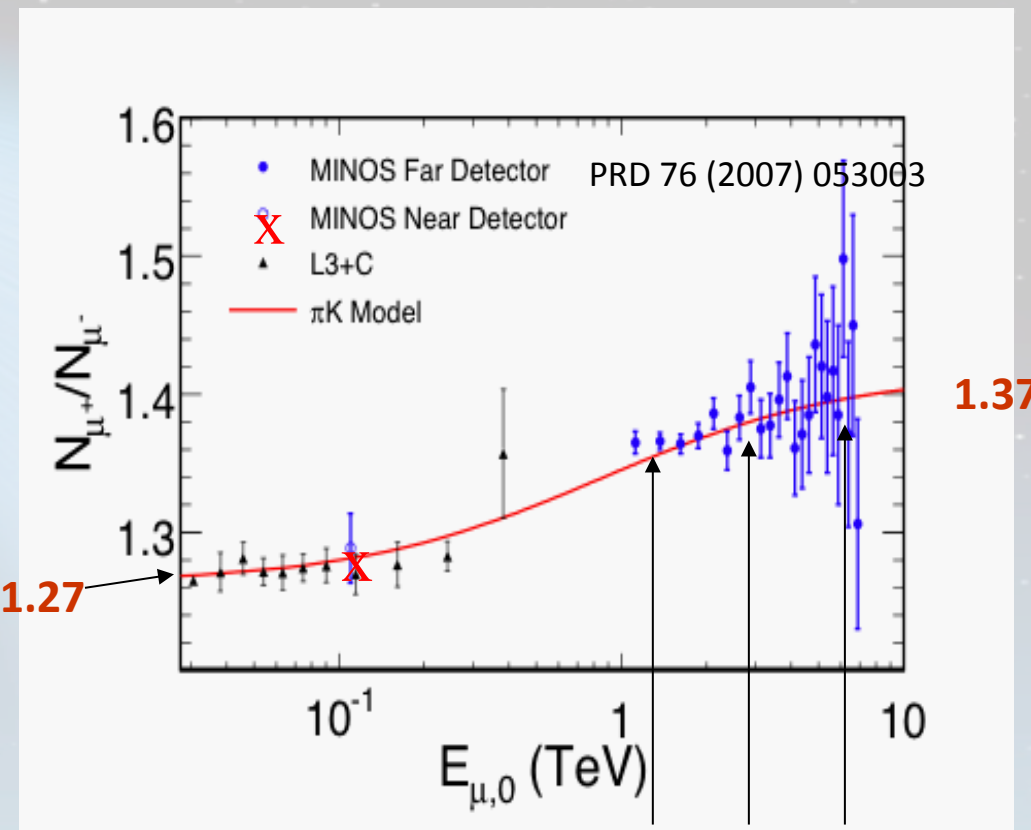
$$\begin{aligned}\mathcal{A} &= \frac{Z_{p\pi^+} - Z_{p\pi^-}}{Z_{p\pi^+} + Z_{p\pi^-}} \\ \mathcal{B} &= \frac{1 - Z_{pp} - Z_{pn}}{1 - Z_{pp} + Z_{pn}}\end{aligned}$$

It is larger than 1 due to:

- An excess of protons on top of the atmosphere
- A steeply falling spectrum

Muon Charge Ratio upto TeV scale

- 100 to 400 GeV at depth
→ > TeV at production
- Increase in charge ratio shows
 - $p \rightarrow K^+ \Lambda$ is important
 - Forward process



Muon Relevance

- Muons background for many experiments
- Atmospheric neutrino flux has same origin as atmospheric muon flux
- Knowledge of muon flux gives precision on atmospheric neutrino flux

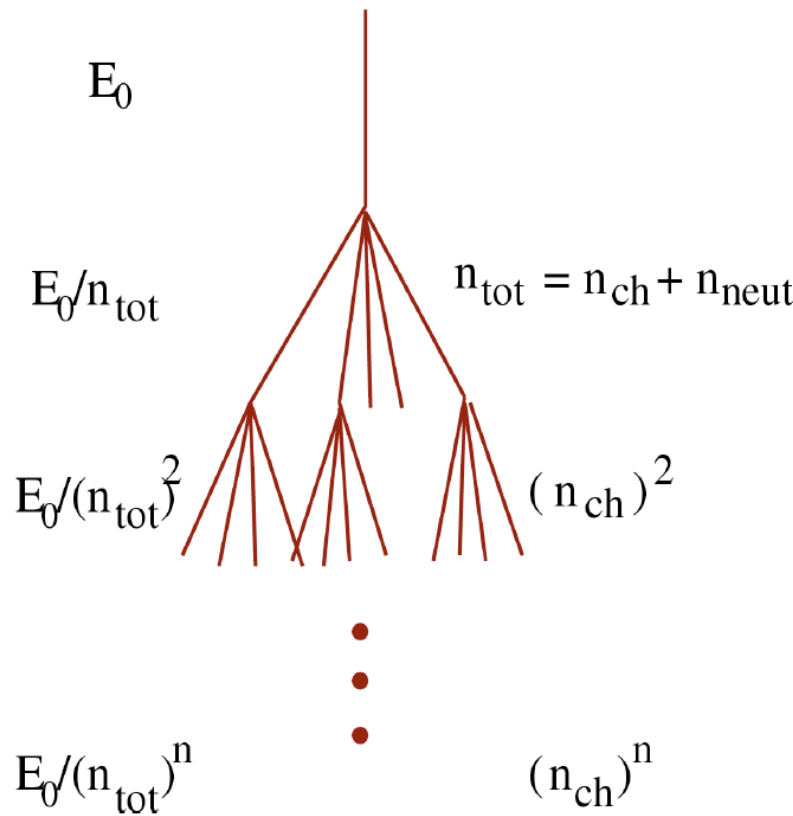


Hadron Showers

Remarks

- It is the same as before, but different boundary conditions
- In reality: Simulation through Monte Carlo (CORSIKA, AIRES)
- Some general comments though

Muon production in had. showers



Primary particle: proton

π^0 decay immediately

Only charged pions initiate new hadronic cascades

Cascade ends with decay at energy E_{dec}

$$E(X) = E_0 / (n_{\text{tot}})^n = E_{\text{dec}}$$

$$N_\mu = (n_{\text{ch}})^n$$

$$N_\mu = \left(\frac{E_0}{E_{\text{dec}}} \right)^\alpha, \quad \alpha = \frac{\ln n_{\text{ch}}}{\ln n_{\text{tot}}} \approx 0.82 \dots 0.95$$

C. Timmermans, Ravelingen BND

Application: superposition model

Proton shower characteristics:

$$N_{max} = E_0/E_c \quad N_\mu = \left(\frac{E_0}{E_{dec}} \right)^\alpha$$
$$X_{max} = \lambda_e \ln(E_0)$$

Assumption:

nucleus of mass A and energy E_0 acts
like A independent nucleons with energy $E_n = E_0/A$

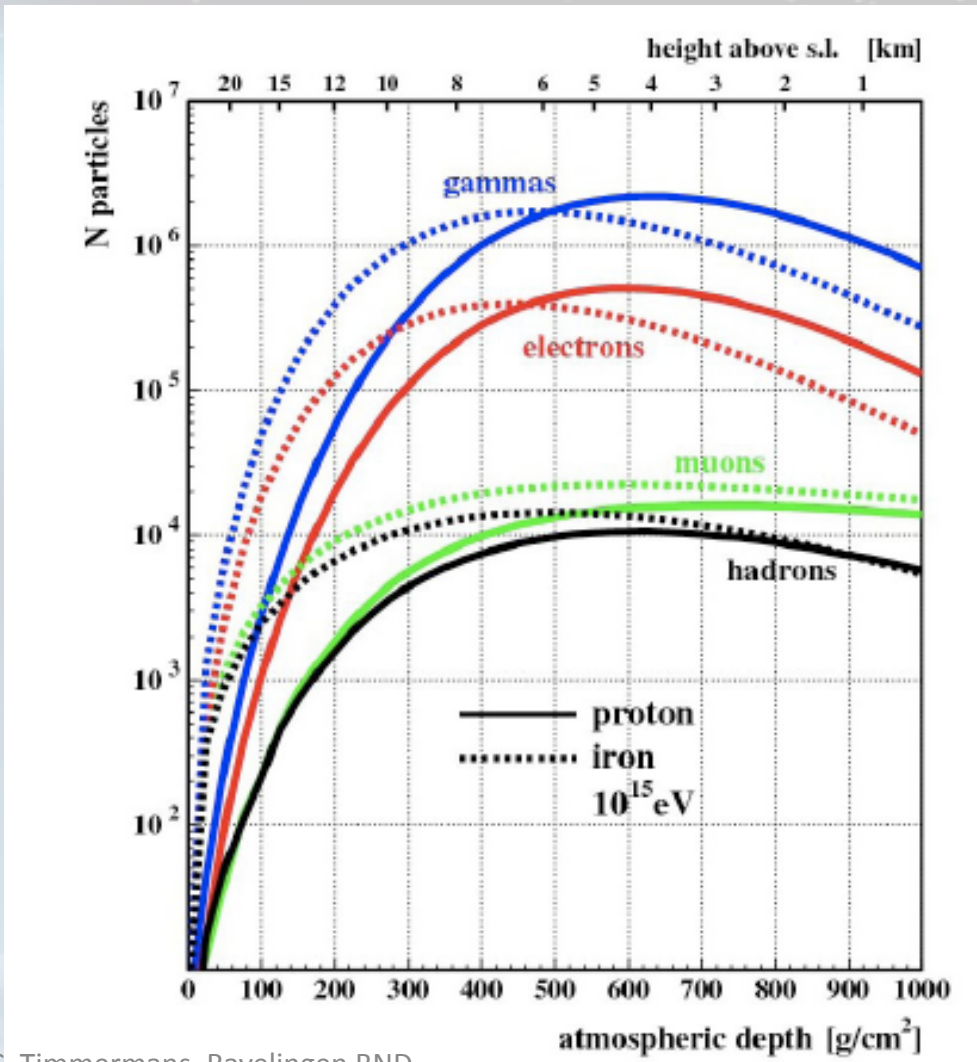
$$N_{max}^A = A E_n/E_c = E_0/E_c$$

$$X_{max}^A \sim \lambda_e \ln(E_0/A)$$

$$N_\mu^A = A \left(\frac{E_0/A}{E_{dec}} \right)^\alpha = A^{1-\alpha} N_\mu$$

Longitudinal Development of Air Showers

Note:
Many more electrons
and photons than
muons and hadrons



Fluorescence detection

- Basic idea:
 - Charged particles in air showers excite nitrogen in atmosphere
 - Nitrogen emits fluorescence light in 300-430 nm range
 - Number of photons proportional to energy deposited in the atmosphere
 - Measure rate as function of slant depth (X) provides longitudinal development profile: (dE/dX)

Absolute Fluorescence yield

- Measured with ^{90}Sr source (Nagano 2004):
 - 5.05 ± 0.71 photons/MeV
- Pressure, temperature dependencies measured in accelerator experiment (AIRFLY, 2007)

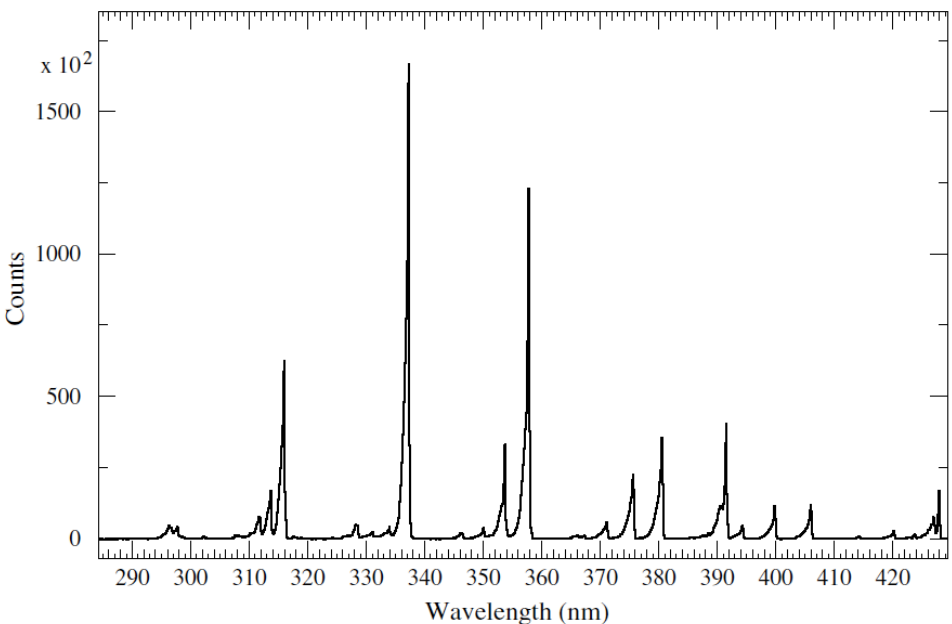


Fig. 4. Measured fluorescence spectrum in dry air at 800 hPa and 293 K.

Fluorescence detector

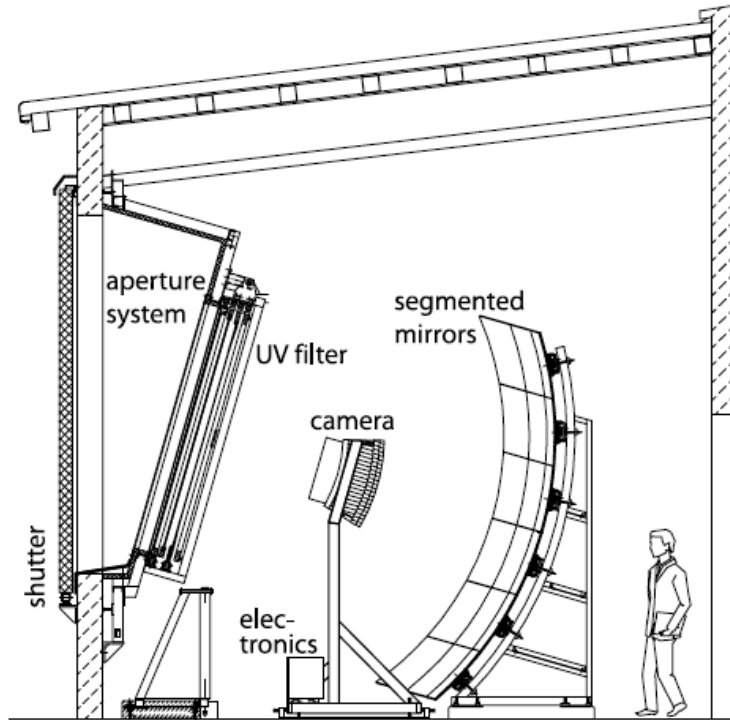
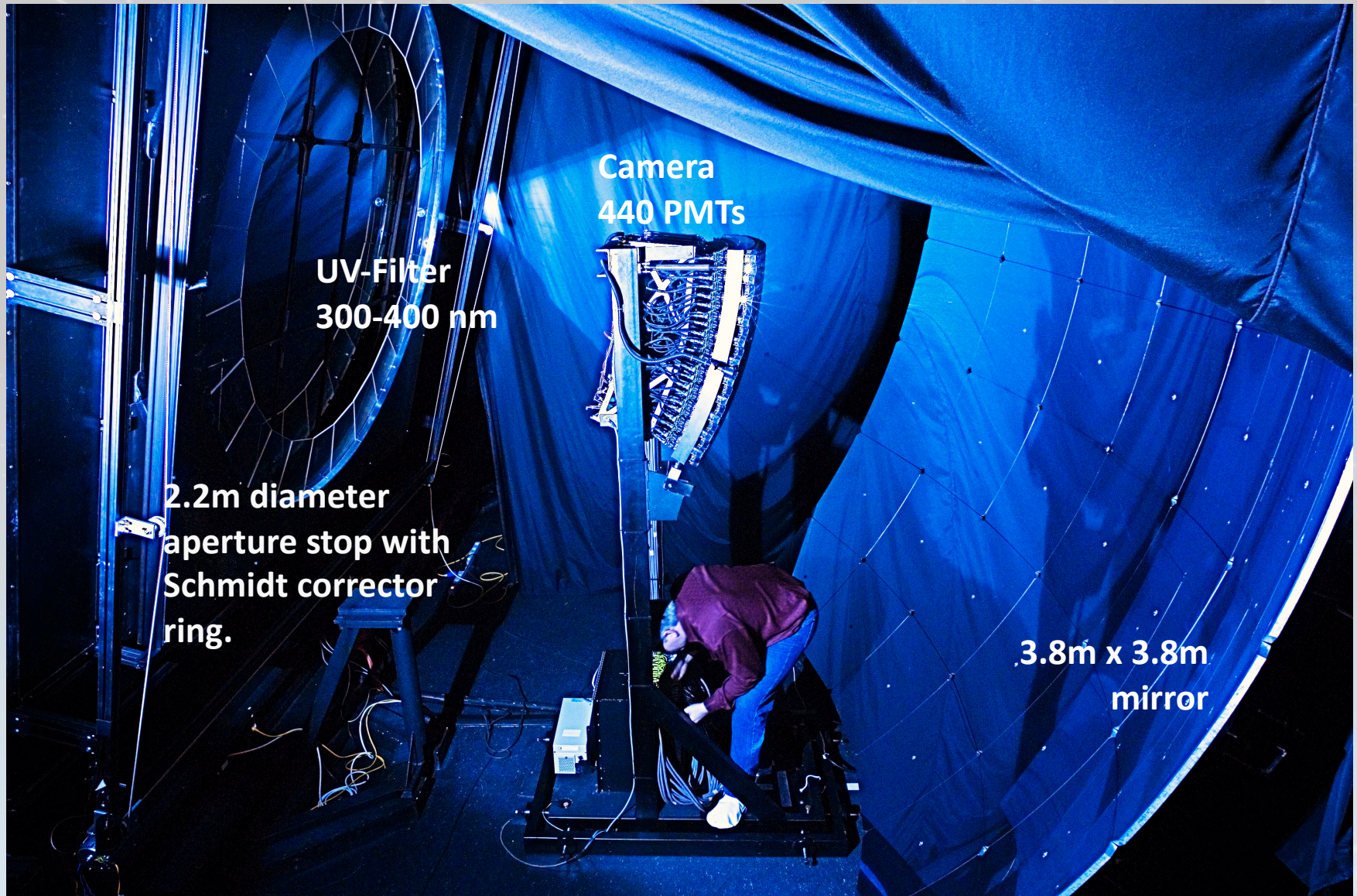


Figure 3: Schematic view of a fluorescence telescope of the Pierre Auger Observatory.



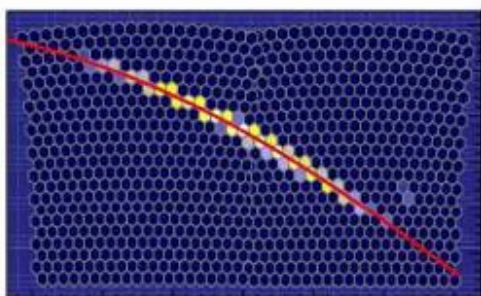
7 sept. 2010

C. Timmermans, Ravelingen BND

Event view:

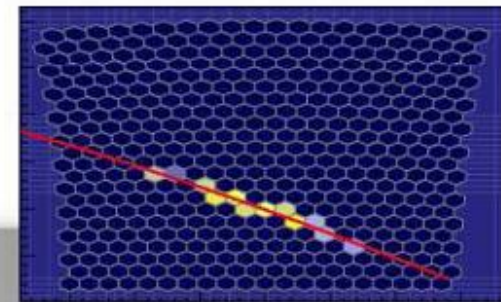
Event: 1364365

Los Morados

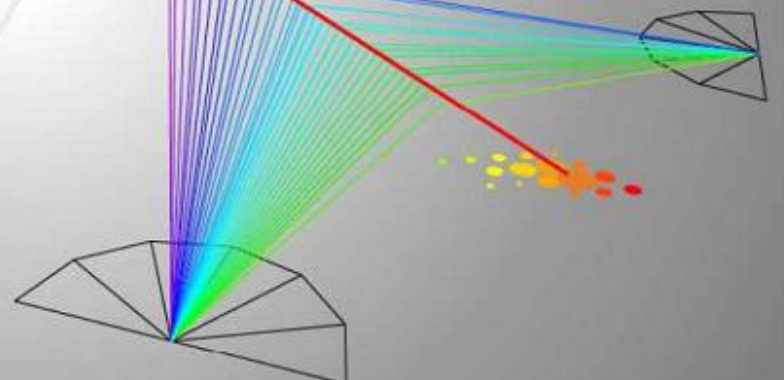


Los Leones

$\lg(E/eV) \sim 19.3$
 $(\theta, \varphi) = (63.7, 148.3)$ deg



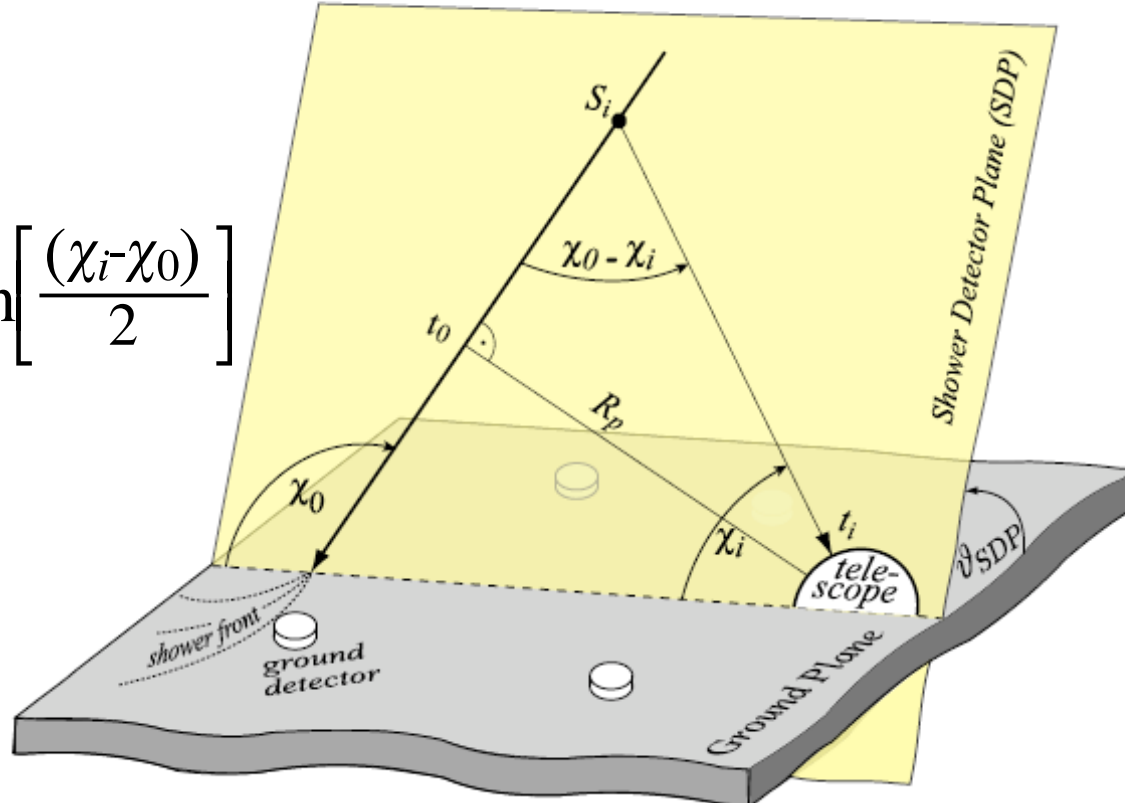
$\lg(E/eV) \sim 19.2$
 $(\theta, \varphi) = (63.7, 148.4)$ deg



SD array: $\lg(E/eV) \sim 19.1$
 $(\theta, \varphi) = (63.3, 148.9)$ deg

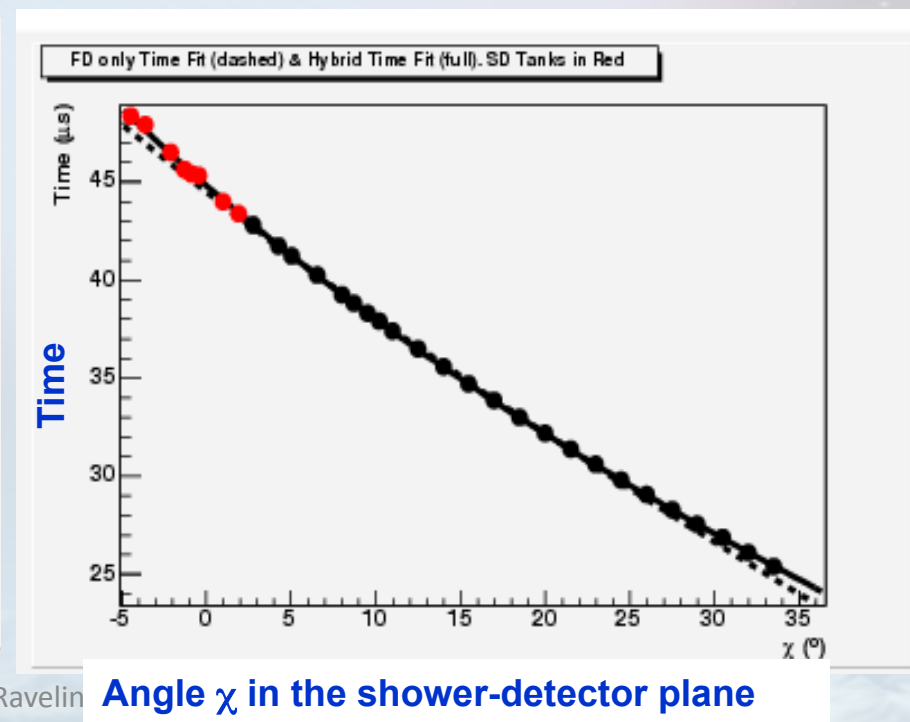
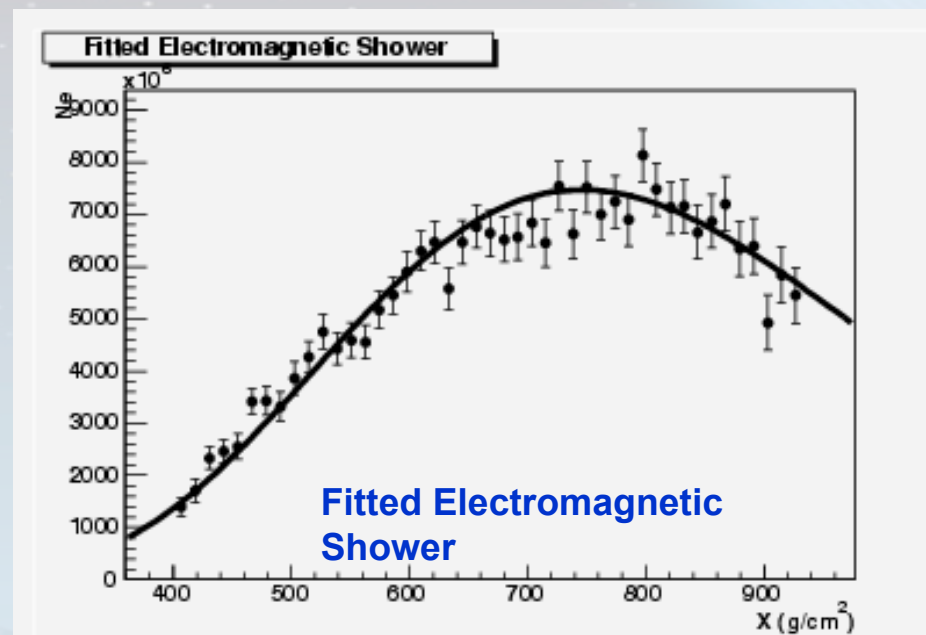
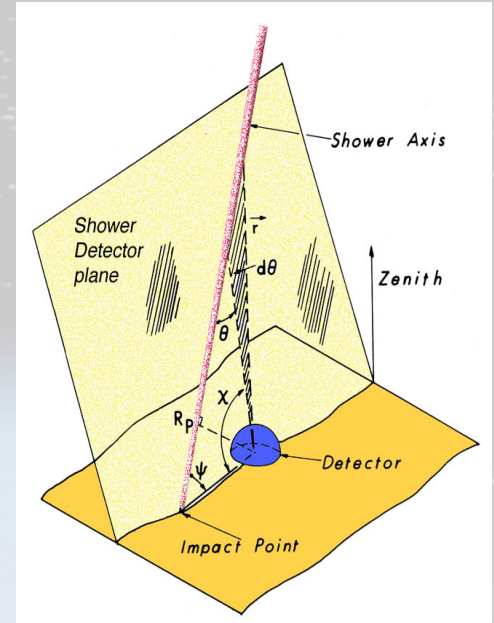
Geometrical shower Reconstruction

$$t_i = t_0 + \frac{R_p}{c} \tan\left[\frac{(\chi_i - \chi_0)}{2}\right]$$

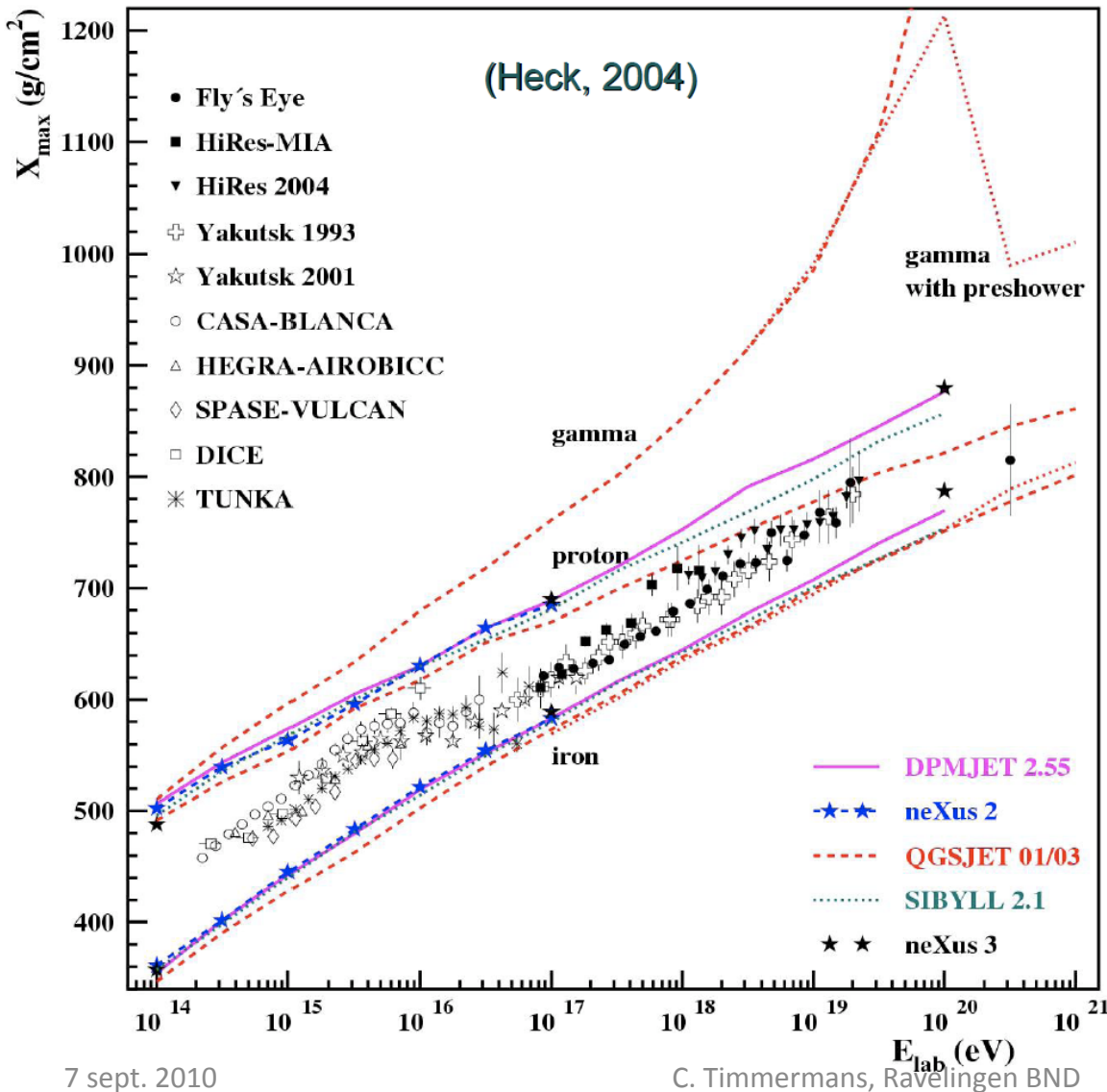


Example Event

*A hybrid event – 1021302
Zenith angle $\sim 30^\circ$, Energy ~ 8 EeV*



Mean depth of shower maximum



Superposition model:

$$X_{max}^A \sim \lambda_e \ln(E_0/A)$$

MC simulation (CORSIKA):

predictions depend on had.
interaction model used for
simulation

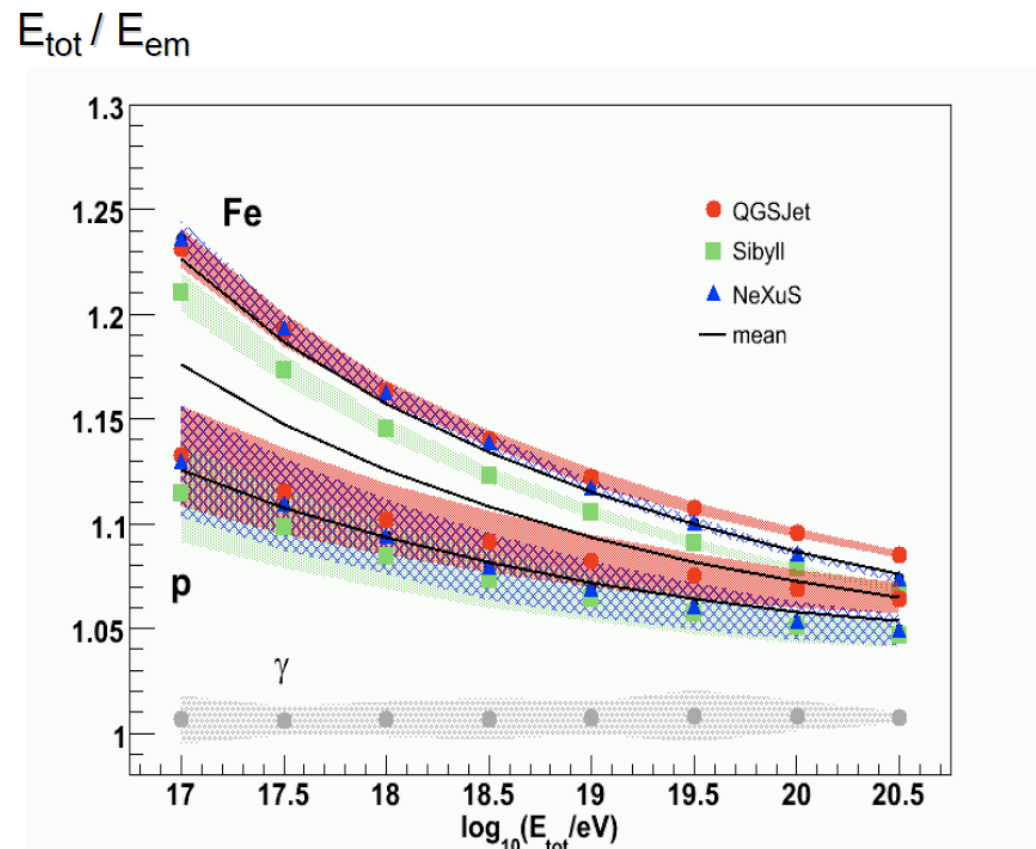
Fluorescence detector: energy

Simulation:

- E_{cal} : ionization deposit in atmosphere
- perfect shower profile measurement assumed

Fluorescence technique at low energy:

- visible energy correction strongly composition dependent
- energy resolution $\sim 10\%$



(Karlsruhe Auger Group)

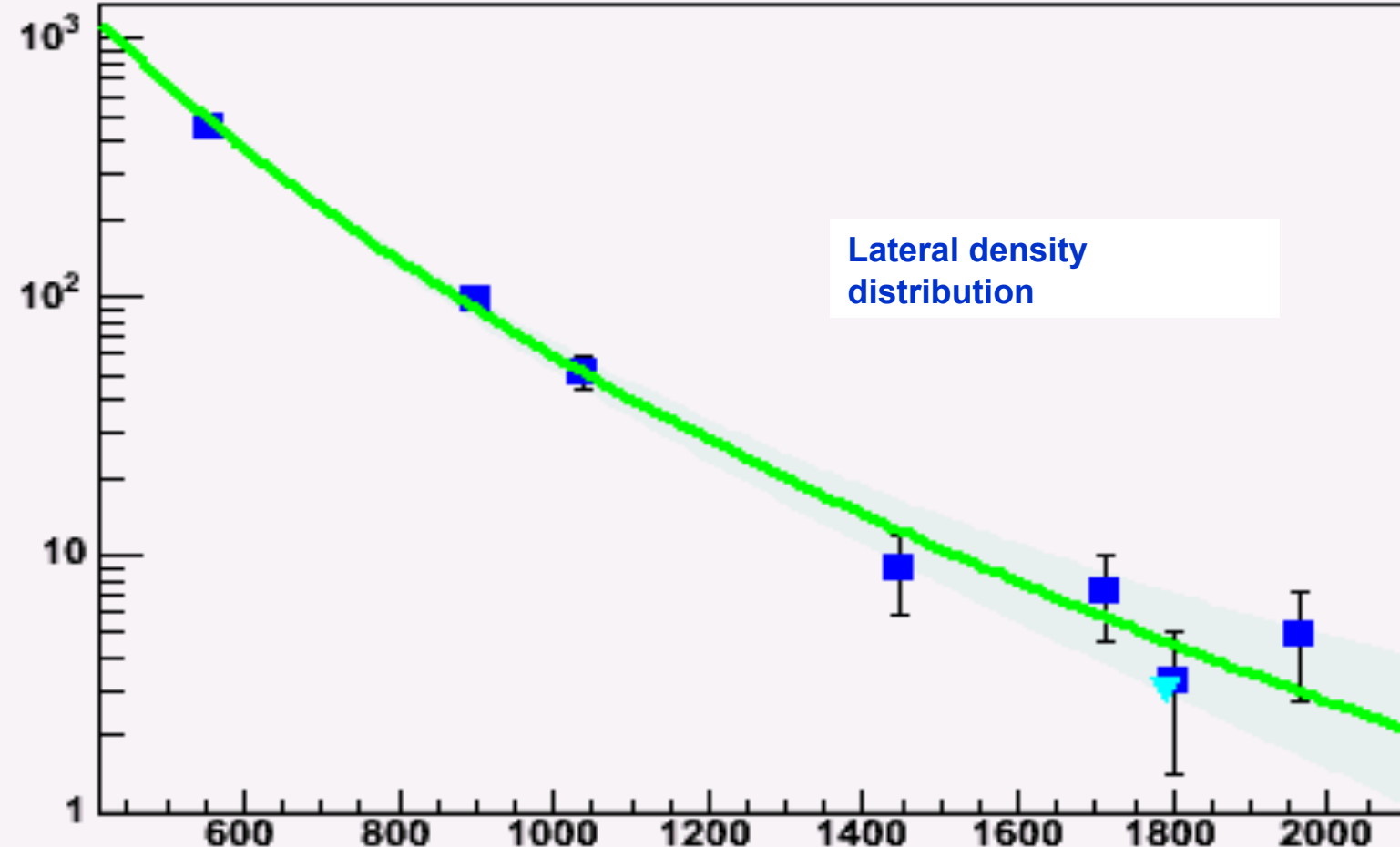
Lateral Distribution of Particles

- NKG-formula (Greisen, Kamata, Nishimura) provide lateral electron distribution as:

$$Q_e = N_e(X) \cdot \frac{C(s)}{r \cdot r_m} \left(\frac{r}{r_m} \right)^{s-1} \left(1 + \frac{r}{r_m} \right)^{s - \frac{9}{2}}$$

- C(s): normalization coefficient
- R_m : Moliere radius. Defined for low energy electrons.
High energy electron distribution smaller: $R_m = R_m E/E_c$
- s: shower age parameter
 - $s < 1$: before shower max
 - $s = 1$: shower max;
 - $s > 1$ after shower max

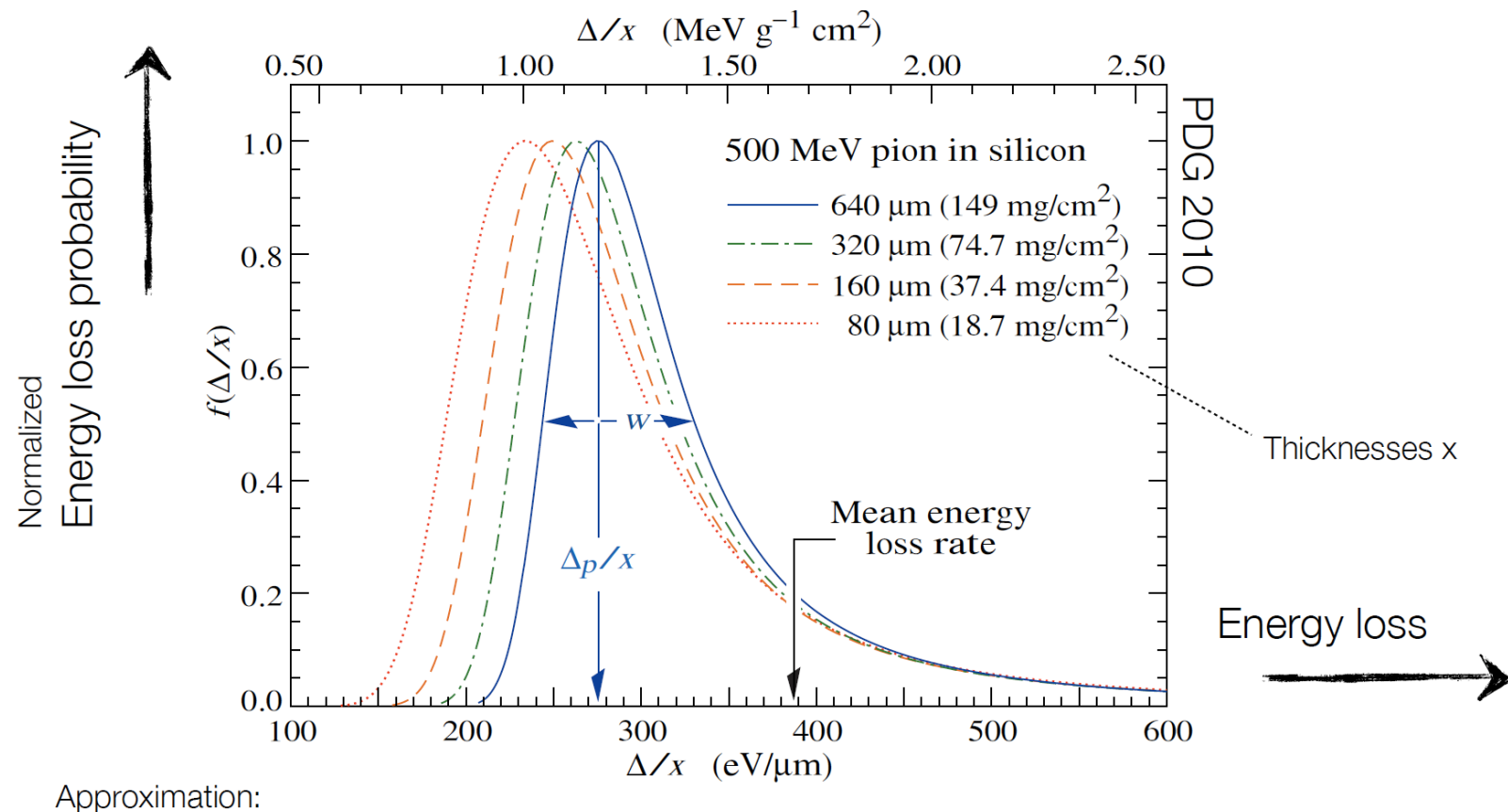
Lateral distribution function fit



Particle Detection

- Basic idea
 - Particle density at surface a measure for shower energy
 - Direction from timing information
 - Curvature a measure for shower development (shower max)
- Standard Detectors:
 - Ionization (scintillator)
 - Cherenkov radiation (water tanks, sea, ice)

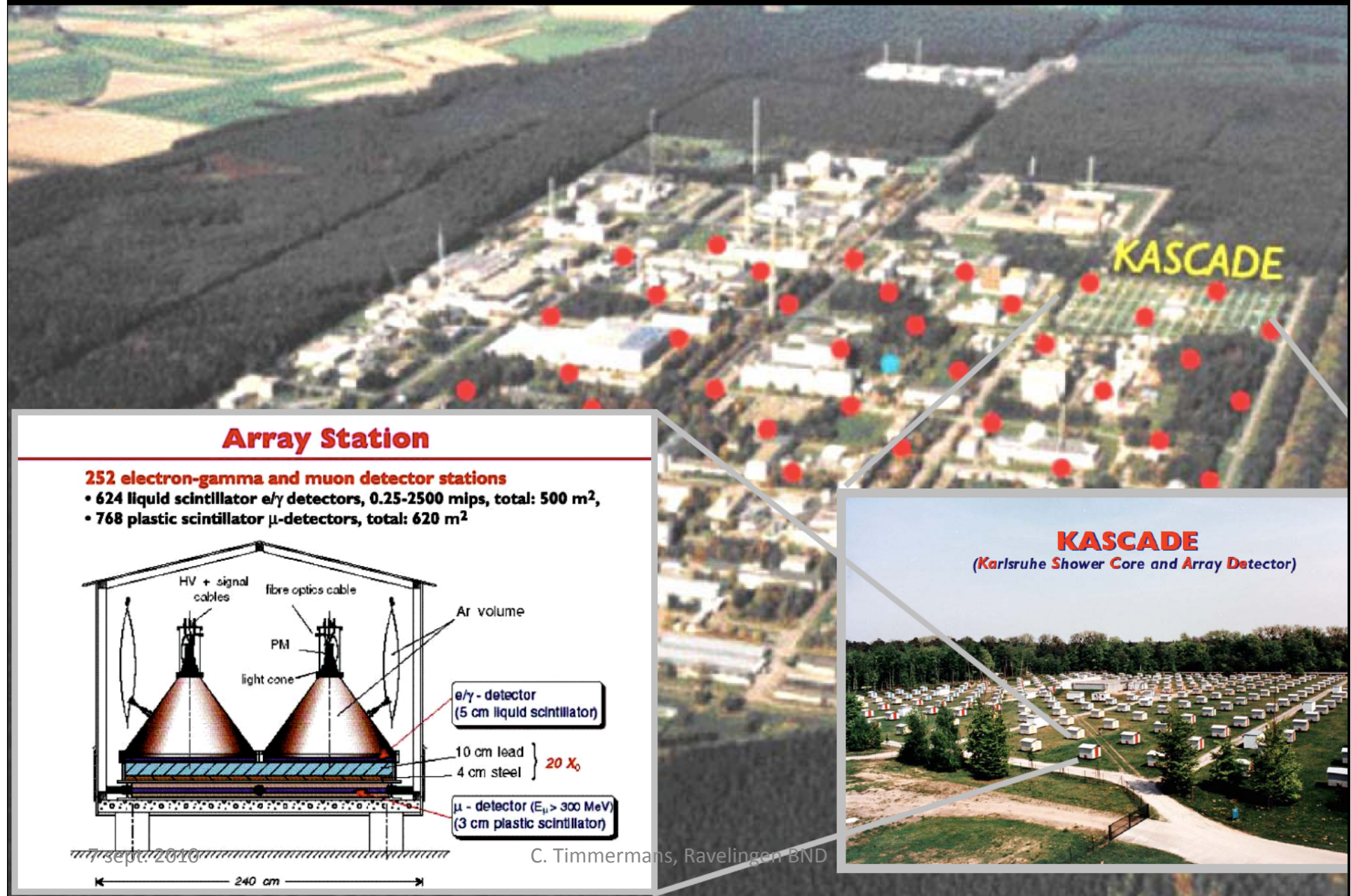
dE/dx Fluctuations – Landau Distribution



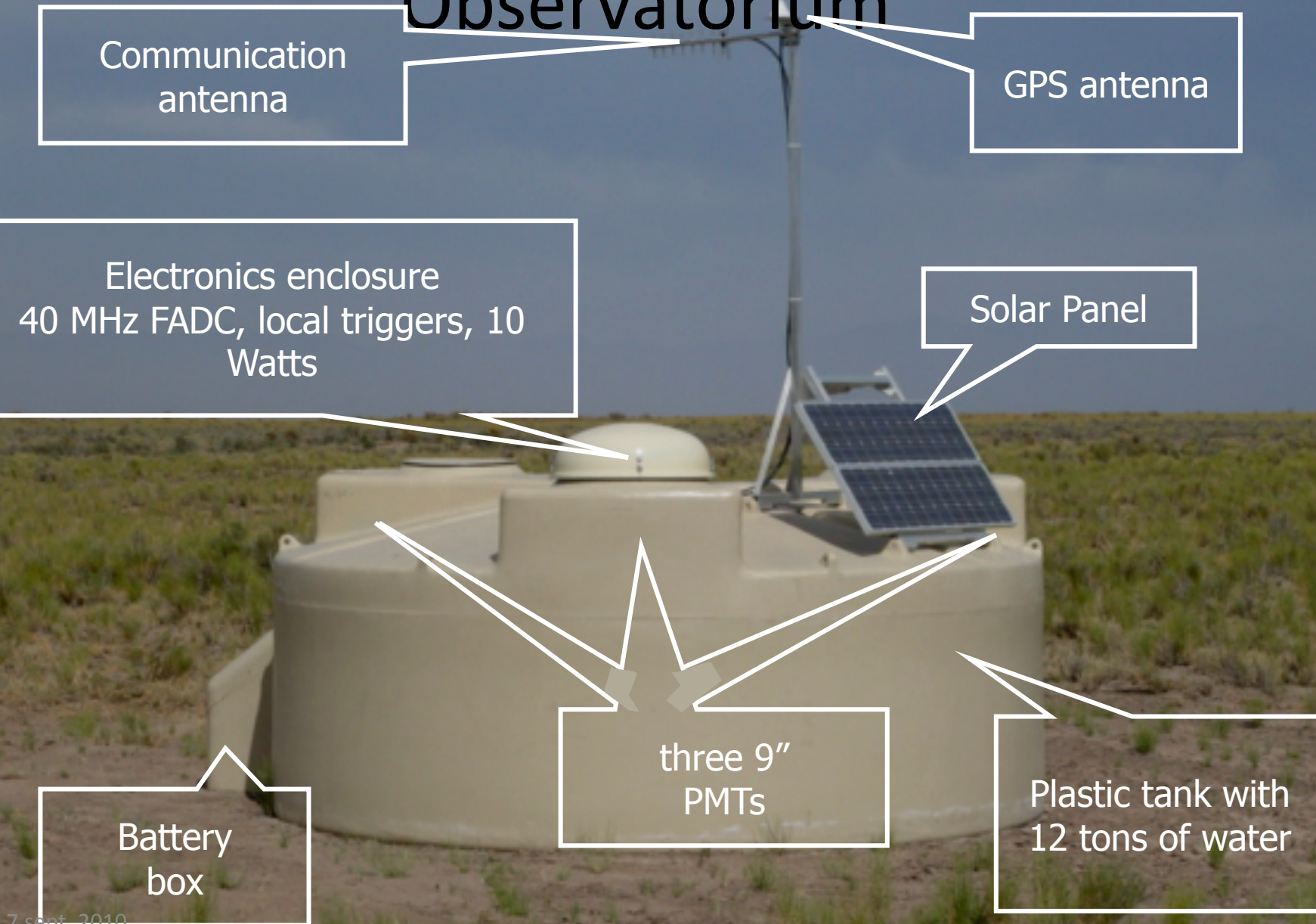
$$f(\Delta/x) = \frac{1}{\sqrt{2\pi}} \exp \left[-\frac{1}{2} \left(\frac{\Delta/x - a(\Delta/x)_{\text{mip}}}{\xi} \right) + e^{-\left(\frac{\Delta/x - a(\Delta/x)_{\text{mip}}}{\xi} \right)} \right]$$

for full form
see e.g. Leo

Airshower detector: KASKADE @ FZ Karlsruhe

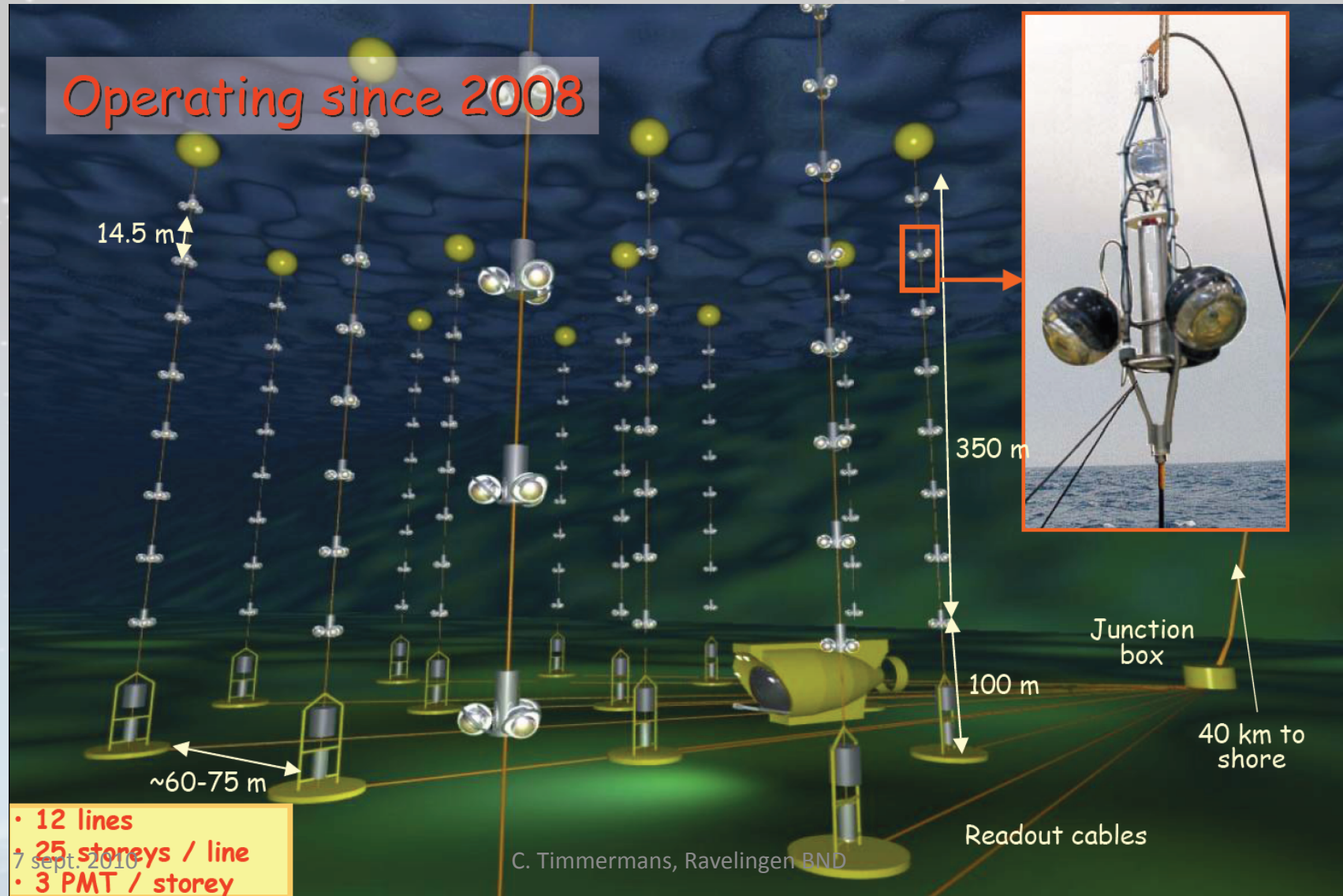


Cherenkov Detector: Pierre Auger Observatorium

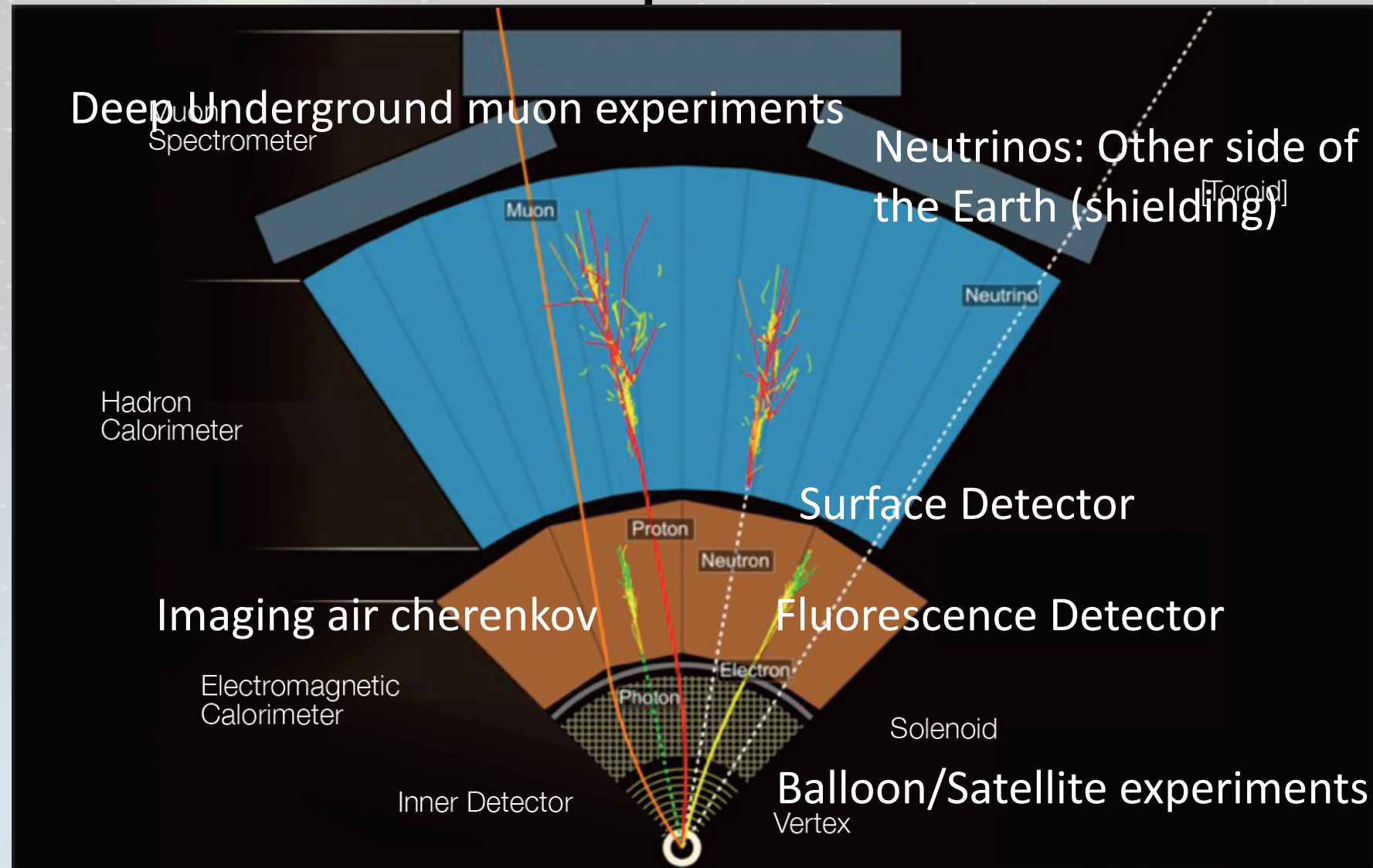


7 sept. 2010

Cherenkov Detector: Antares

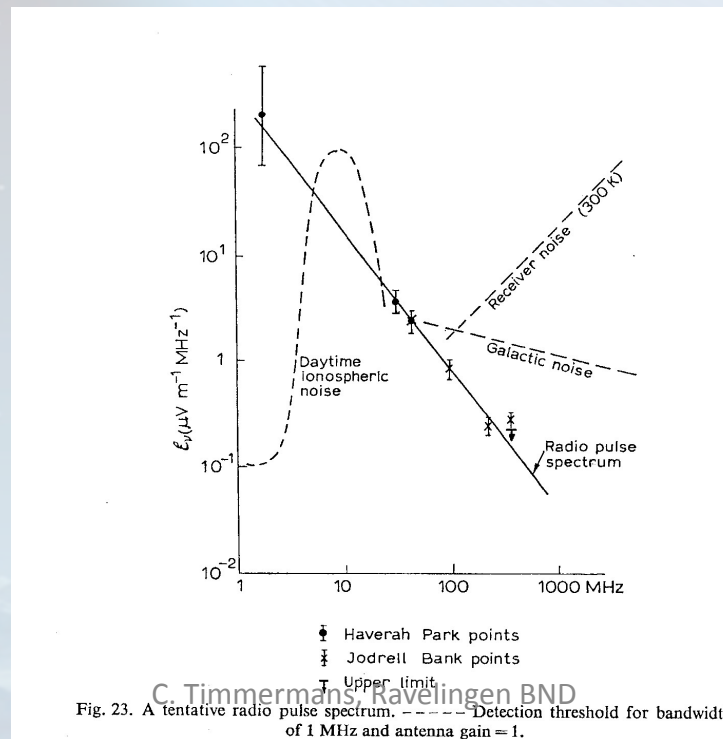
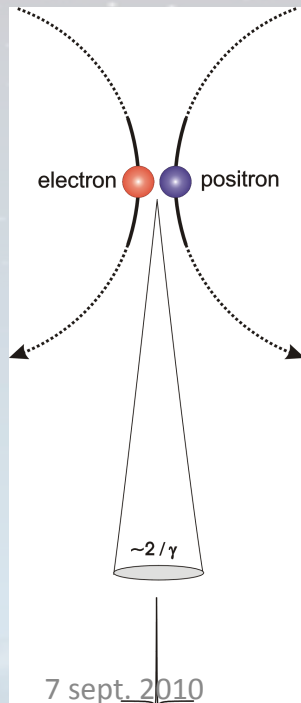


Lets Compare to ATLAS



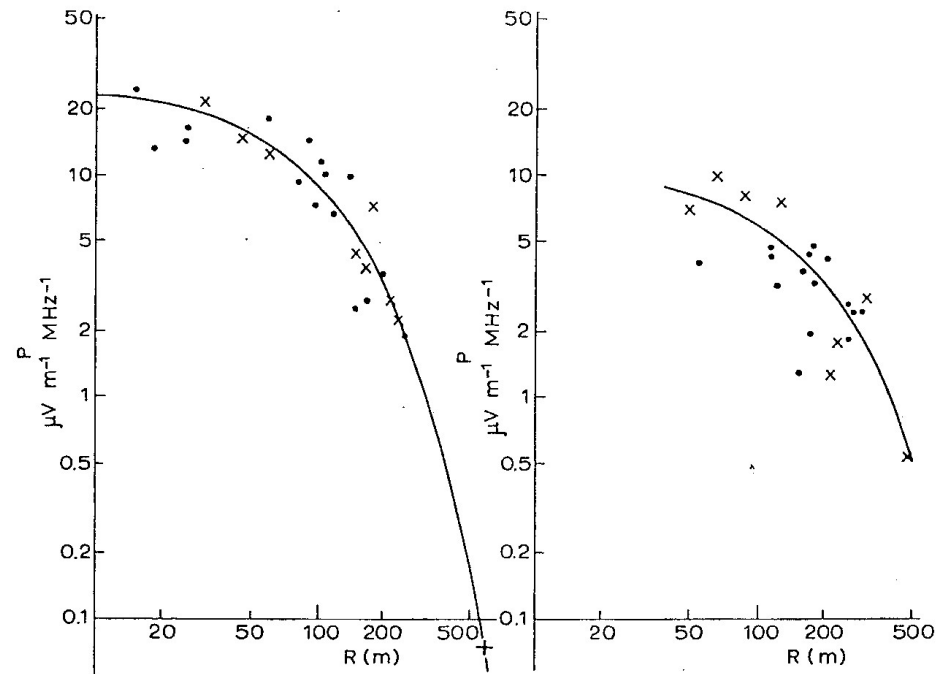
Radio Detection of Air Showers

- Coherent emission of radiation in Air Showers
- Main contribution: Geo-synchrotron
 - Other contributions (may) exist



A window of opportunity
between 20 and 100 MHz

Radio Lateral Distribution

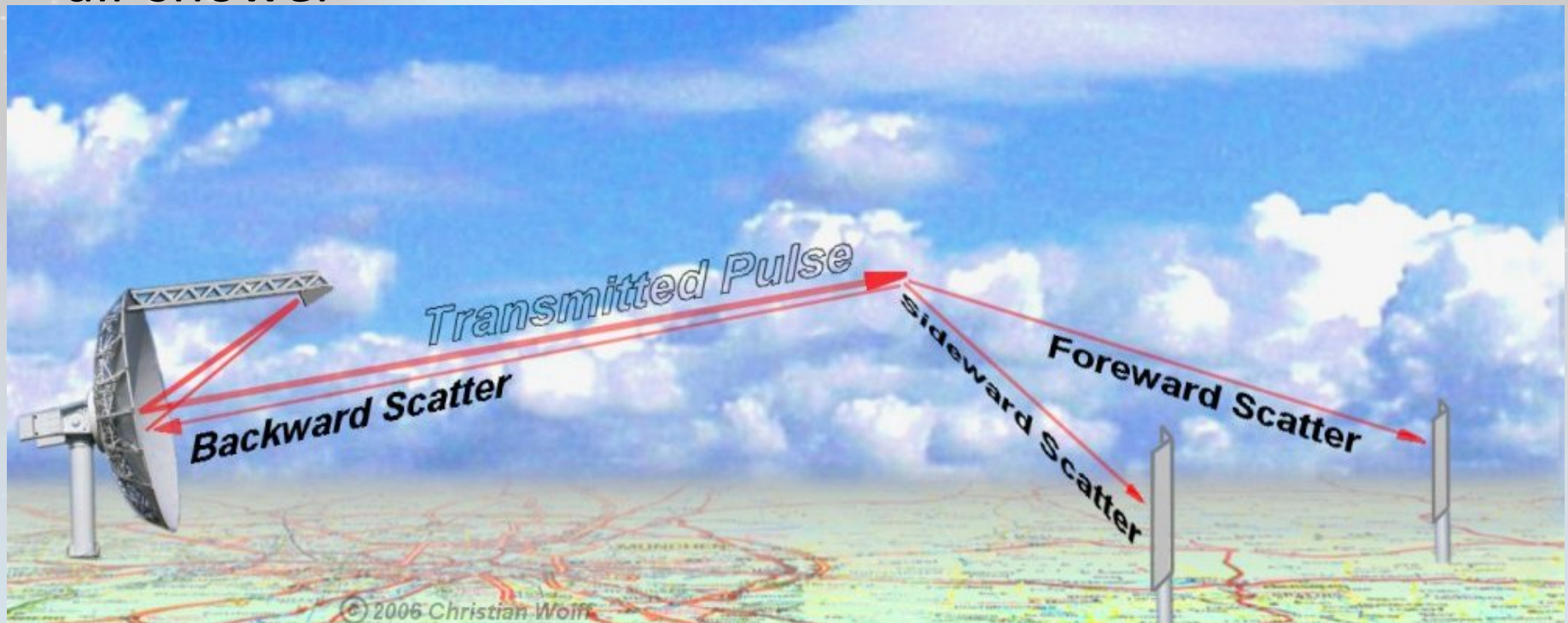


$$\mathcal{E}_v = 20 \left(\frac{E_p}{10^{17}} \right) \sin \alpha \cos \theta \exp \left(-\frac{R}{R_0(v, \theta)} \right) \quad \mu\text{V m}^{-1} \text{ MHz}^{-1}. \quad (84)$$

References p. 296

Bistatic Radar

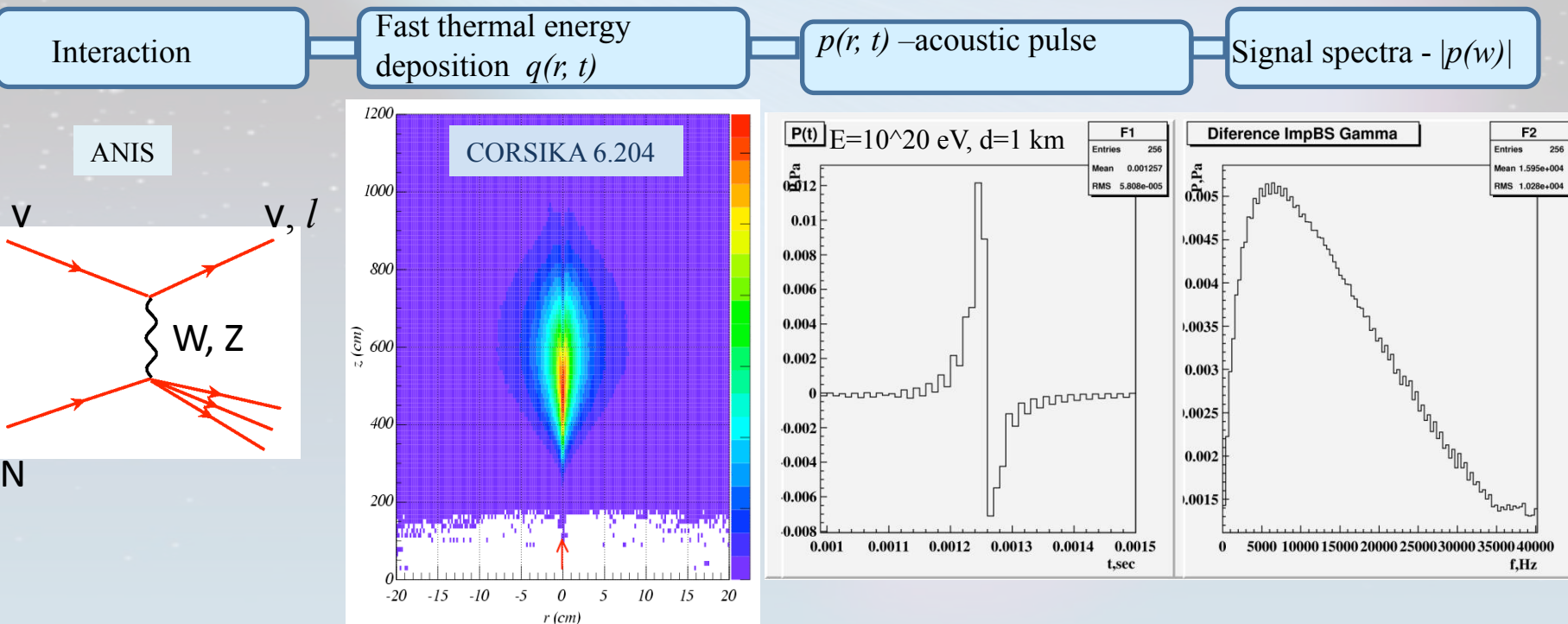
forward scattering off ionization cloud produced by air shower



Acoustic Detection

Wave equation

$$\nabla^2 p(\vec{r}, t) - \frac{1}{c_s^2} \frac{\partial^2 p(\vec{r}, t)}{\partial t^2} = -\frac{\beta}{C_p} \frac{\partial^2 q(\vec{r}, t)}{\partial t^2} \quad \Rightarrow \quad p(\vec{r}, t) = \frac{\beta}{4\pi \cdot C_p} \int \frac{dV'}{|\vec{r} - \vec{r}'|} \cdot \frac{\partial^2}{\partial t'^2} q\left(\vec{r}', t - \frac{|\vec{r} - \vec{r}'|}{c_s}\right)$$

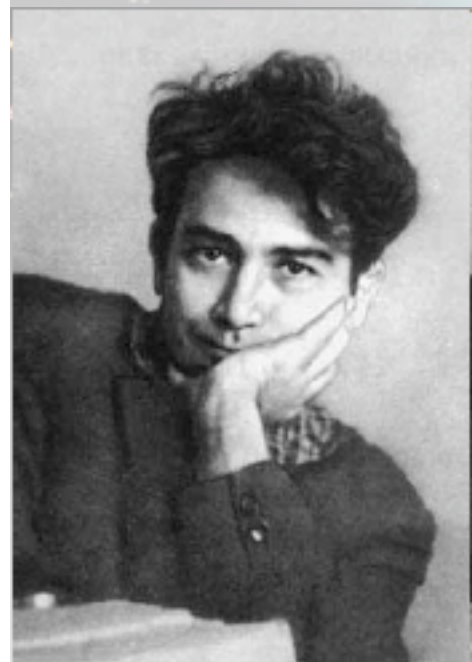


[S. Bevan et al. Simulation of ultra high energy neutrino induced showers in ice and water // Astropart. Phys. 28 (2007) 366.]

7 sept. 2010

C. Timmermans, Ravelingen BND

Acoustic Detection



Гидродинамическое излучение от треков ионизирующих частиц в стабильных жидкостях

G. A. Askaryan

Atomnaja Energija V3(1957)152

Hydrodynamic radiation
from tracks of ionizing
particles in stable liquids

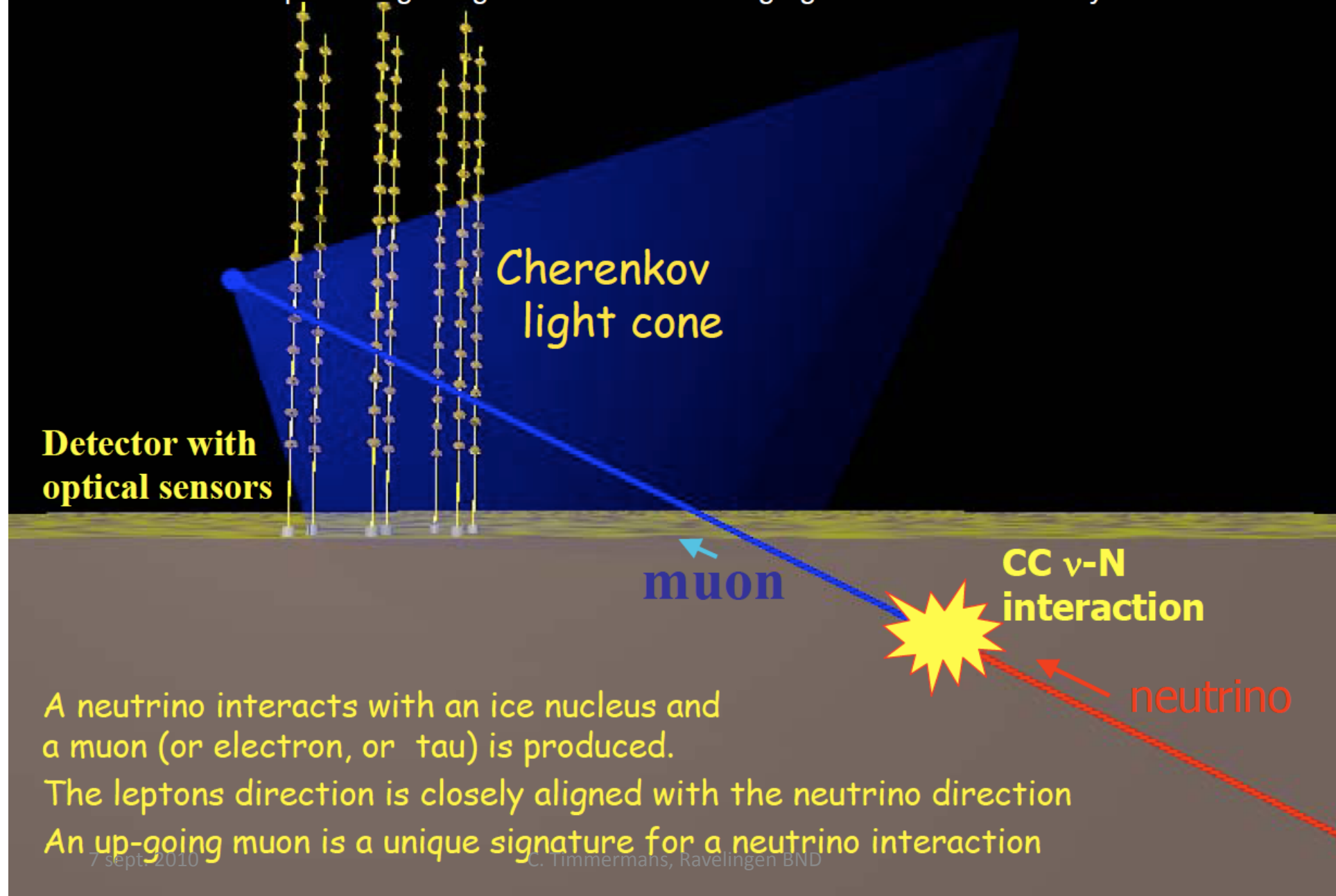
Прохождение ионизирующих частиц в жидкостях сопровождается увлечением молекул среды расталкивающимися скоплениями одноименно заряженных ионов и микровзрывами при локальных нагревах, создаваемых вблизи треков частиц. Эти

The passage of ionizing particles in liquids is accompanied by entrainment of molecules of the medium by mutually repelling accumulations of like-charge ions and microexplosions upon local heating near the particle tracks. These processes

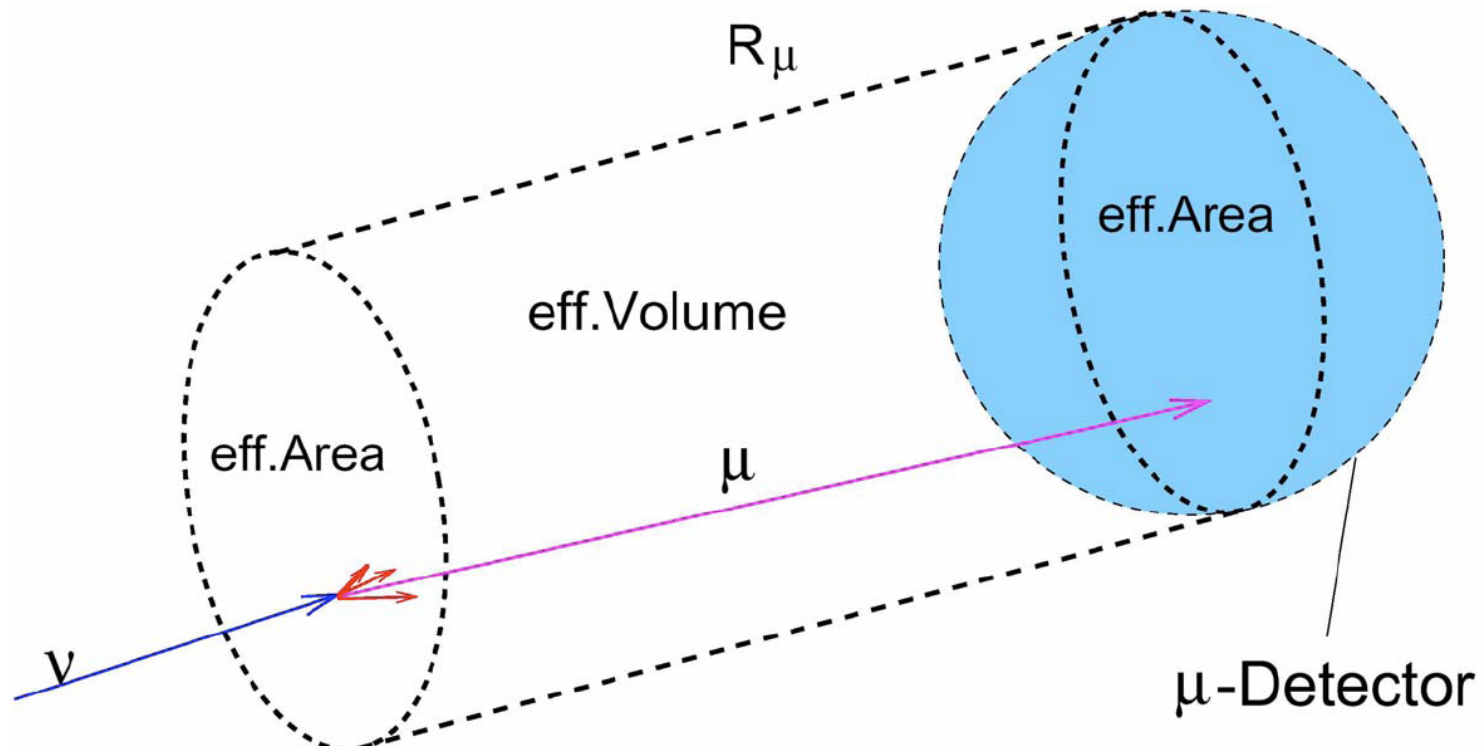
First mentioning of an acoustic particle detection possibility

Neutrino Detection

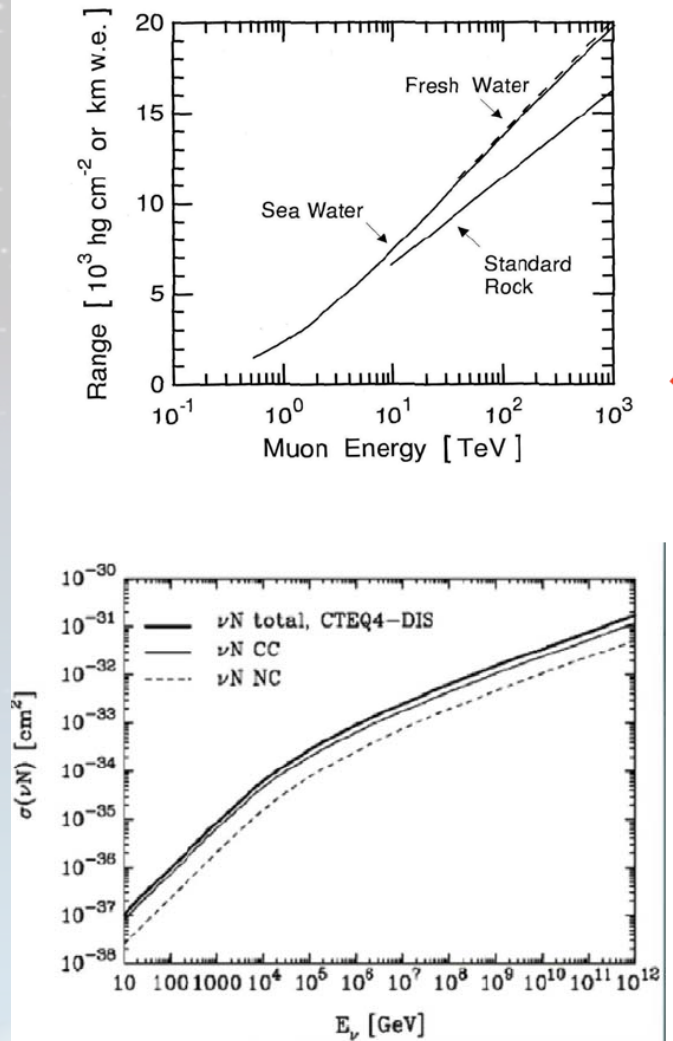
requires large target mass and shielding against other cosmic rays



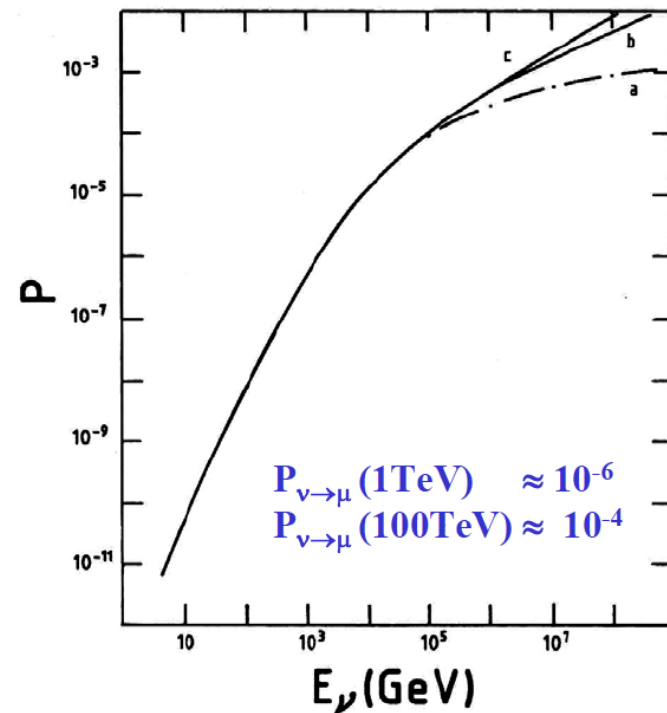
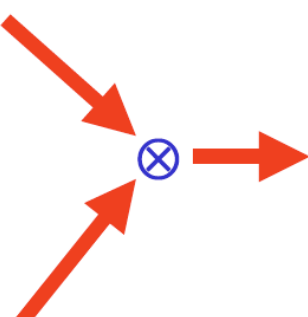
$$V_{\text{eff}} = A_{\text{eff}} \otimes R_\mu$$



Neutrino Detection Probability



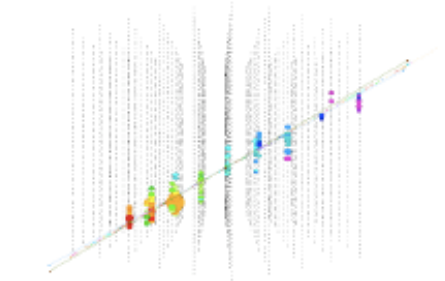
$$N_{event} = A_{eff}(E_\mu) \otimes R_\mu(E_\mu) \otimes \frac{d\sigma(E_\nu)}{dE_\mu} \otimes \frac{d\phi}{dE_\nu}$$



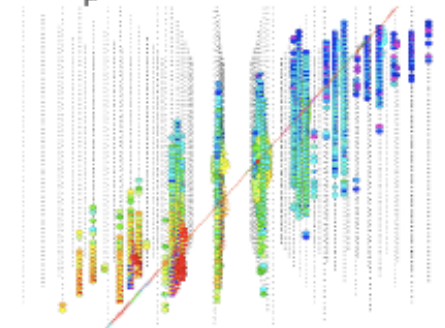
Neutrino Topologies

Muon neutrino

a) $E_\mu = 10 \text{ TeV} \sim 90 \text{ hits}$



b) $E_\mu = 6 \text{ PeV} \sim 1000 \text{ hits}$



$E \sim dE/dx, E > 1 \text{ TeV}$

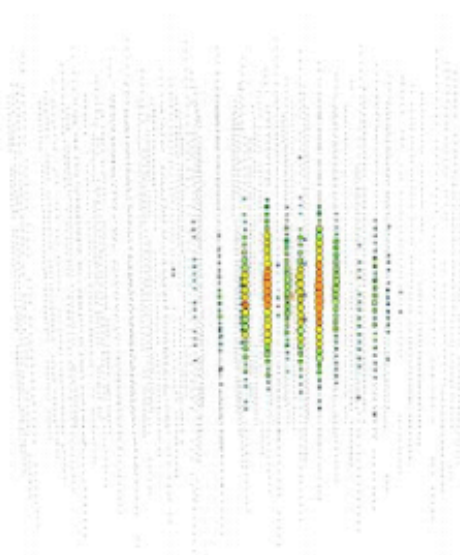
Energy Res. : $\log(E) \sim 0.3$

Angular Res.: 0.8 -2 deg

7 sept. 2010

Electron neutrino

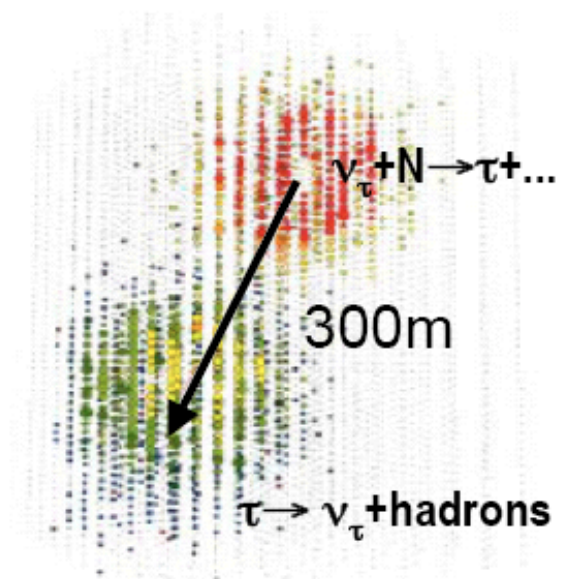
$E = 375 \text{ TeV}$



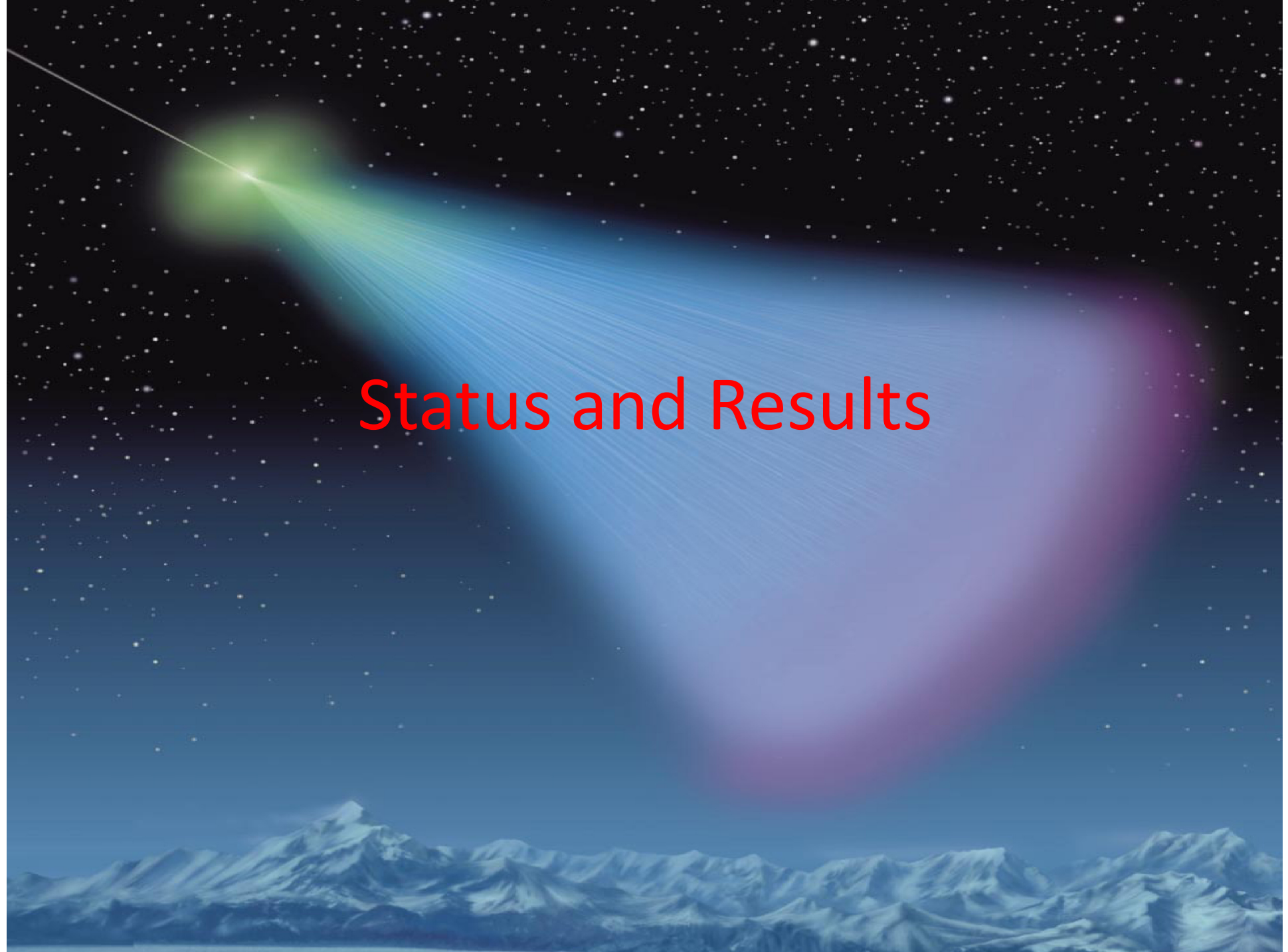
Energy Res. $\log(E) \sim 0.1-0.2$
Poor Angular Resolution
C. Timmermans, Ravelingen BND

Tau neutrino

$E = 10 \text{ PeV}$

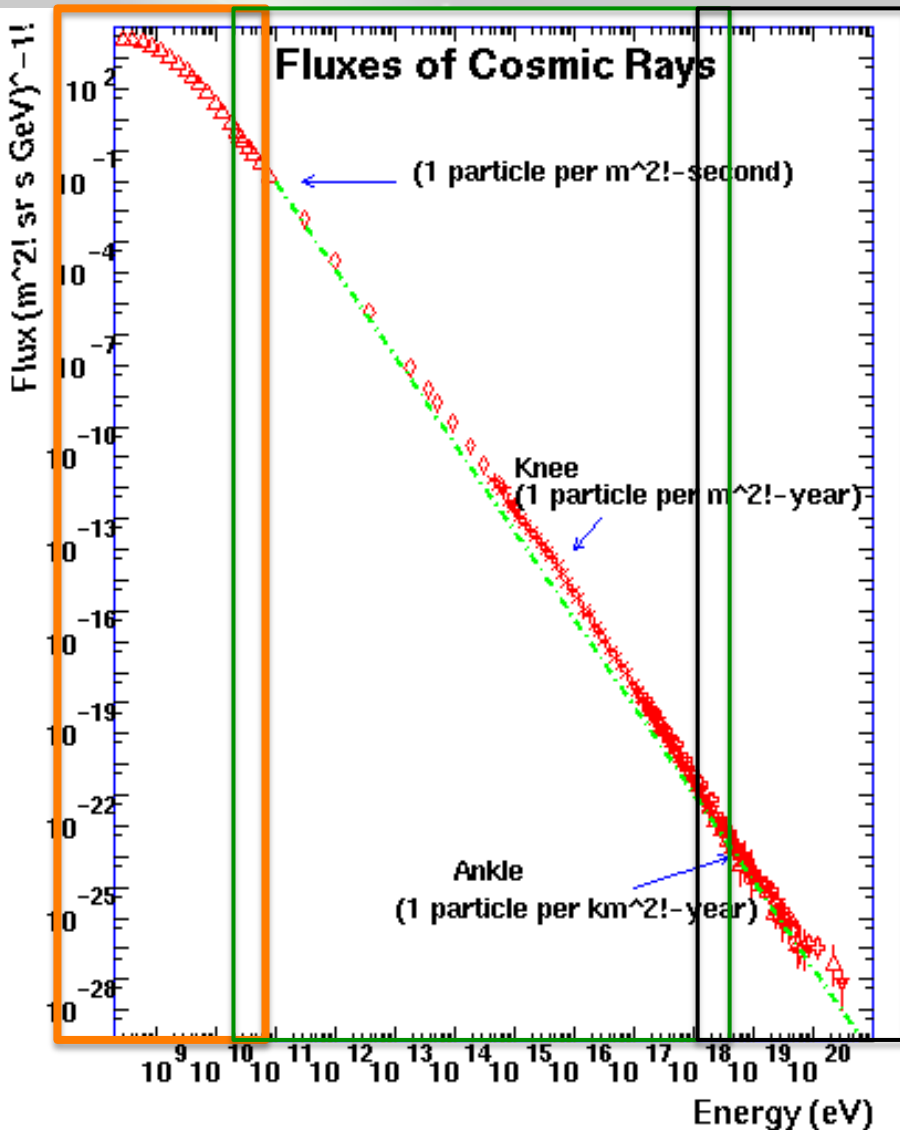


Double-bang signature
above $\sim 1 \text{ PeV}$
Very low background
Pointing capability
Best energy measurement



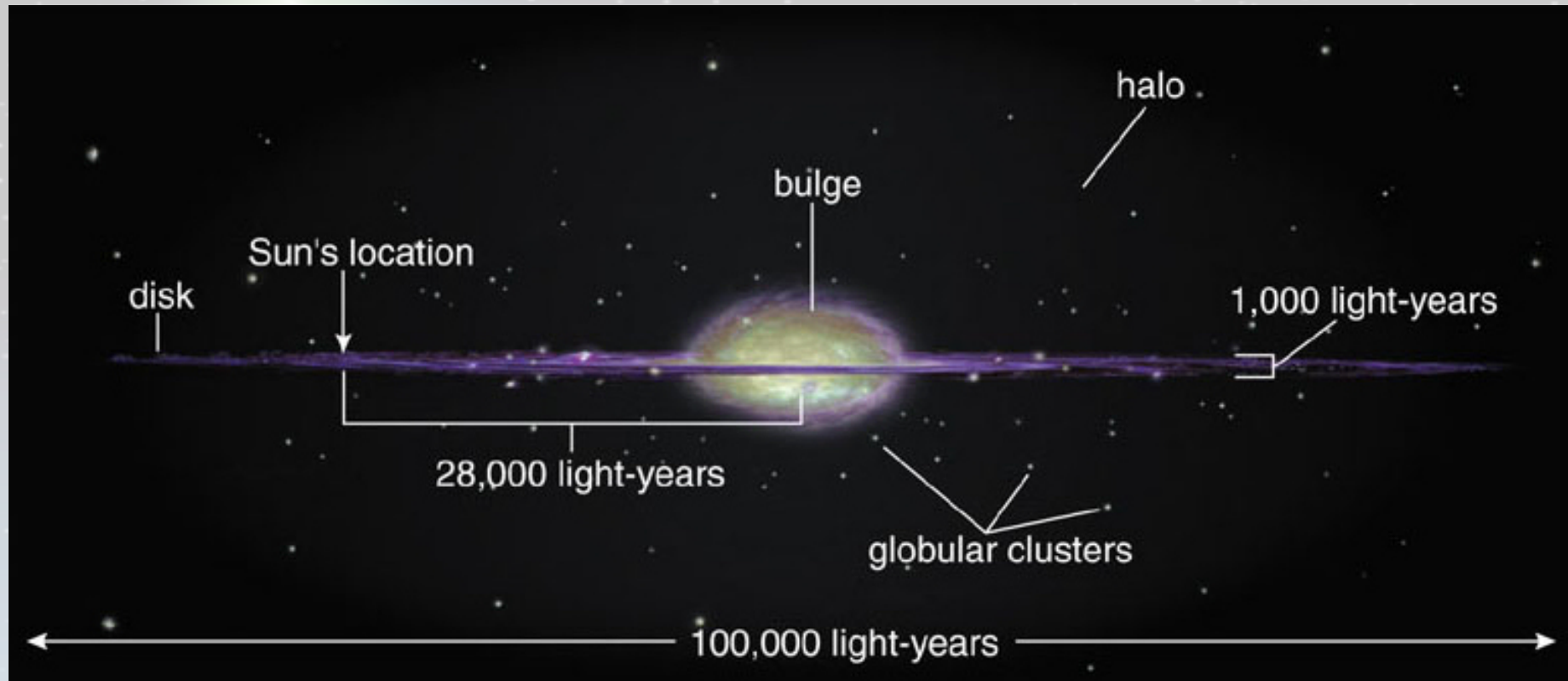
Status and Results

Fluxes of Cosmic Rays



- Below $\sim 10^{11}$ eV:
Solar Modulation
- Below $\sim 10^{18}$ eV:
Galactic origin
- Highest energies:
Extra galactic

Let's set the scale



$$1 \text{ AU} = 1.5 \cdot 10^{11} \text{ m}$$

$$1 \text{ ly} = 9.5 \cdot 10^{15} \text{ m} = 6.3 \cdot 10^4 \text{ AE}$$

$$1 \text{ pc} = 3.1 \cdot 10^{16} \text{ m} = 3.26 \text{ ly}$$

Magnetic fields in space

Solar system magnetic field: $\sim 10 \mu\text{G}$

The Galactic magnetic field: $\sim 1 \mu\text{G}$ (eg Zeeman splitting spectral lines)

The intergalactic field: $\sim 1\text{-}100 \text{ nG}$

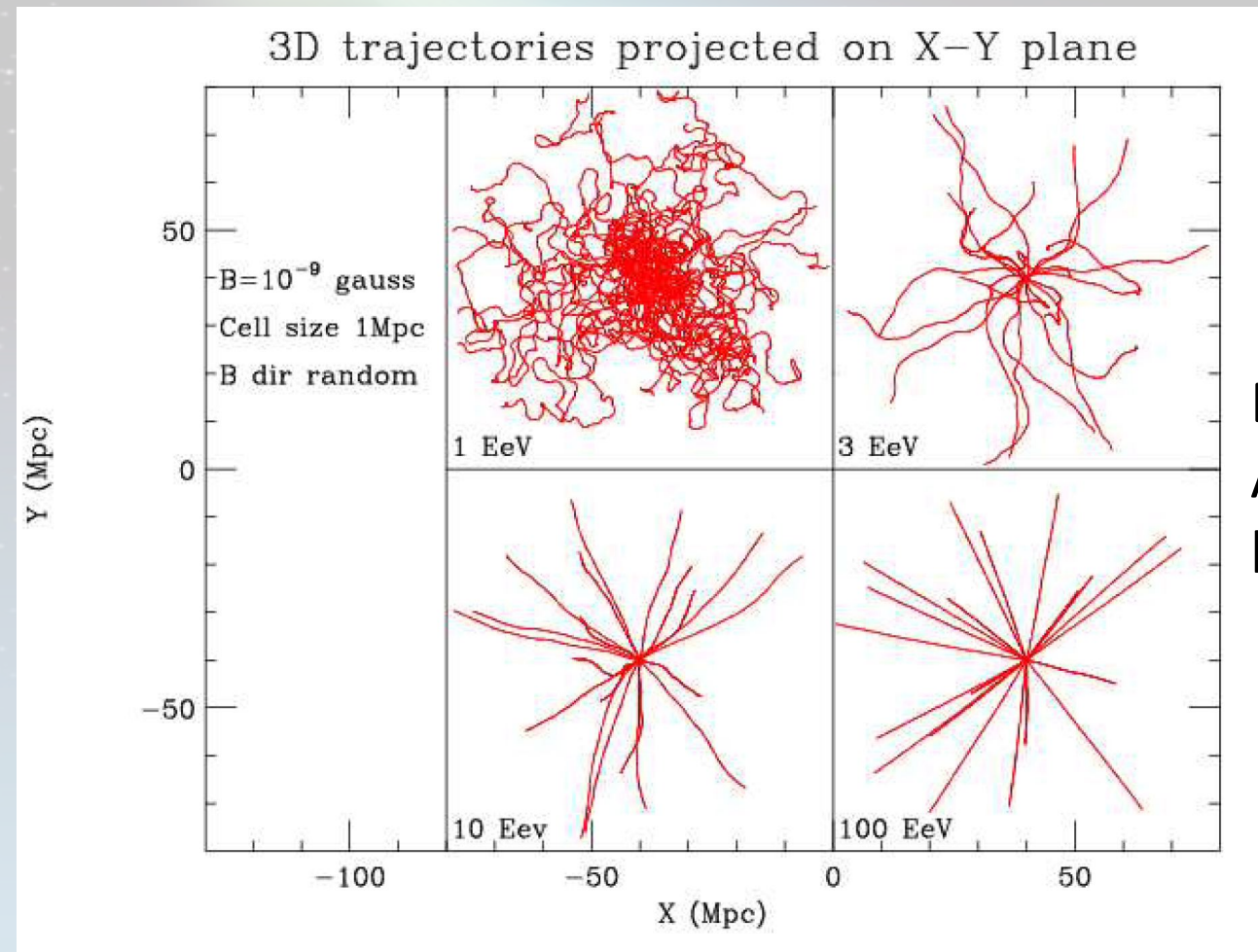
$$R_{\text{gyro}} = p/qB = 2 \cdot 10^2 (p/1\text{TeV})/B(\mu\text{G}) \text{ (a.u.)}$$

$$R_{\text{gyro}} = 0.1 (p/1\text{PeV})/B(\mu\text{G}) \text{ (kpc)}$$

→ Above several TeV no deflection in solar system

→ Above 10^{16} eV extragalactic enter

Bending of Cosmic Rays



Expect:
All Rays are scrambled
by B-fields

Below the knee: TeV CR

- Main active detectors:
 - Milagro (wide view gamma detector)
 - Icecube (neutrino detector)
 - SuperKamiokande
 - Tibet Air Shower Array

Comparison of Gamma-Ray Detectors

Low Energy Threshold
EGRET/GLAST



Space-based (Small Area)
“Background Free”
Large Duty Cycle/Large Aperture

Sky Survey (< 10 GeV)
AGN Physics
Transients (GRBs) < 100 GeV

High Sensitivity
HESS, MAGIC, VERITAS



Large Effective Area
Excellent Background Rejection
Low Duty Cycle/Small Aperture

High Resolution Energy Spectra
Studies of known sources
Surveys of limited regions of sky

Large Aperture/High Duty Cycle
Milagro, Tibet, ARGO, HAWC

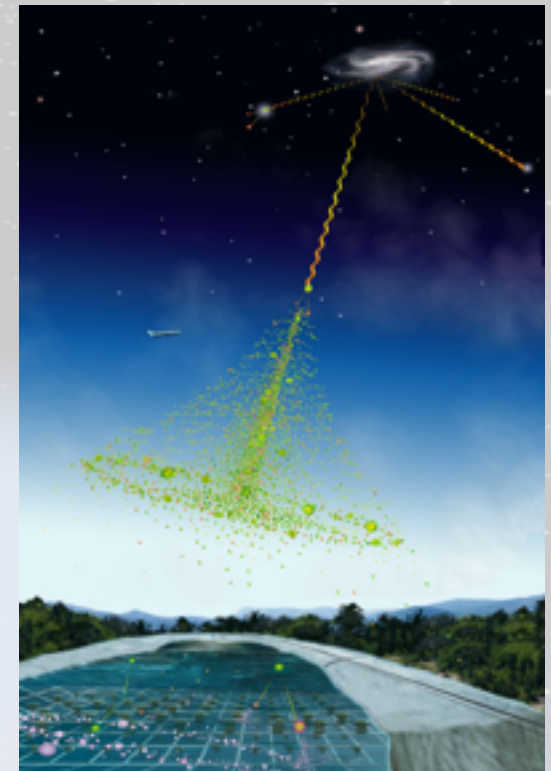
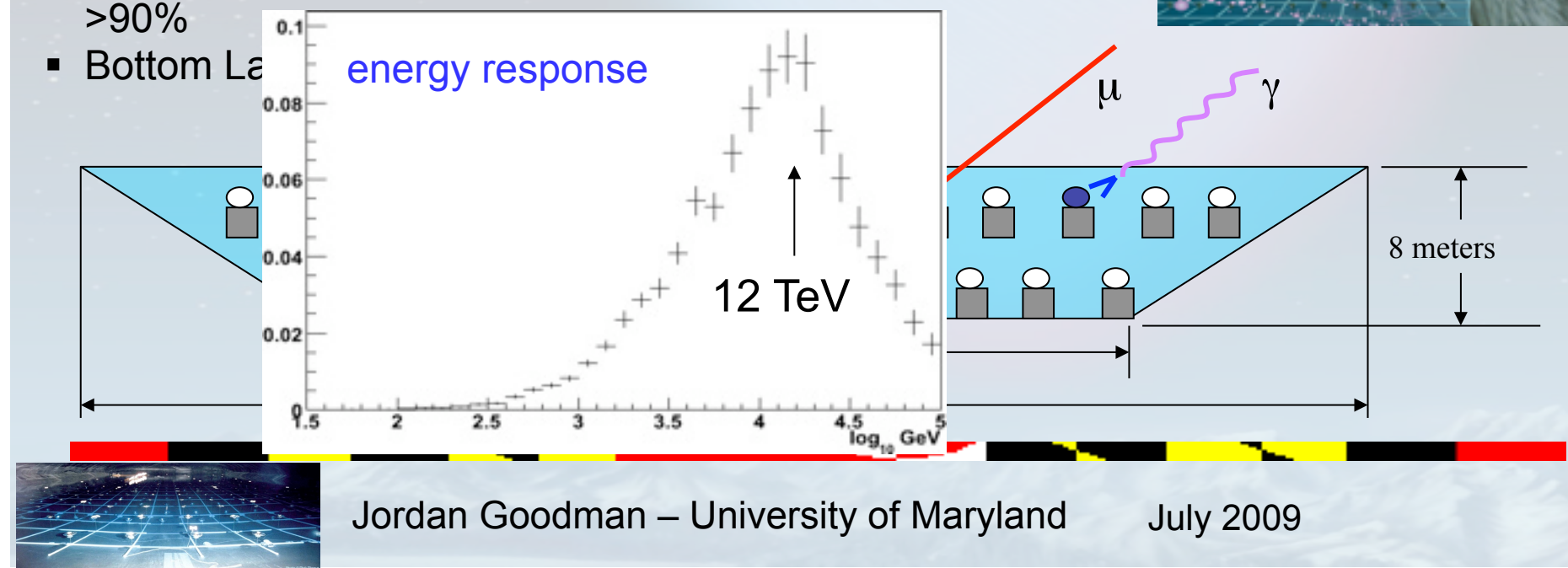


Moderate Area
Good Background Rejection
Large Duty Cycle/Large Aperture

Unbiased Sky Survey
Extended sources
Transients (GRB's)
Solar physics/space weather

How Does Milagro Work?

- Detect Particles in Extensive Air Showers from Cherenkov light created in 60m x 80 m x 8m pond containing filtered water
- Reconstruct shower direction to $\sim 0.5^\circ$ from the time different PMTs are hit
- 1700 Hz trigger rate mostly due to Extensive Air Showers created by cosmic rays
- Field of view is ~ 2 sr and the average duty factor is $>90\%$
- Bottom La



Inside the Milagro Detector



Photo © Rick Dingus



Jordan Goodman – University of Maryland

July 2009

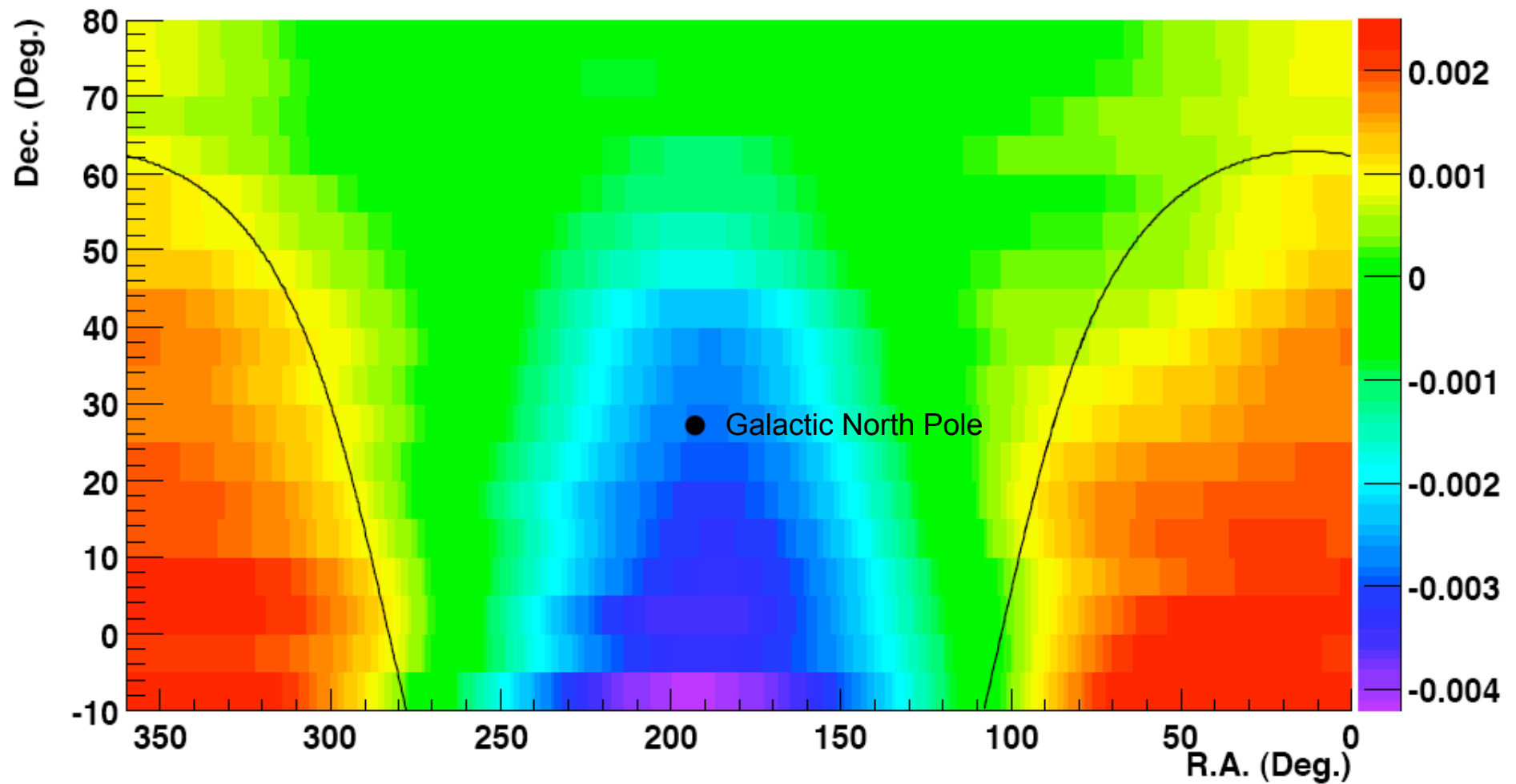


Array of 175 Outriggers

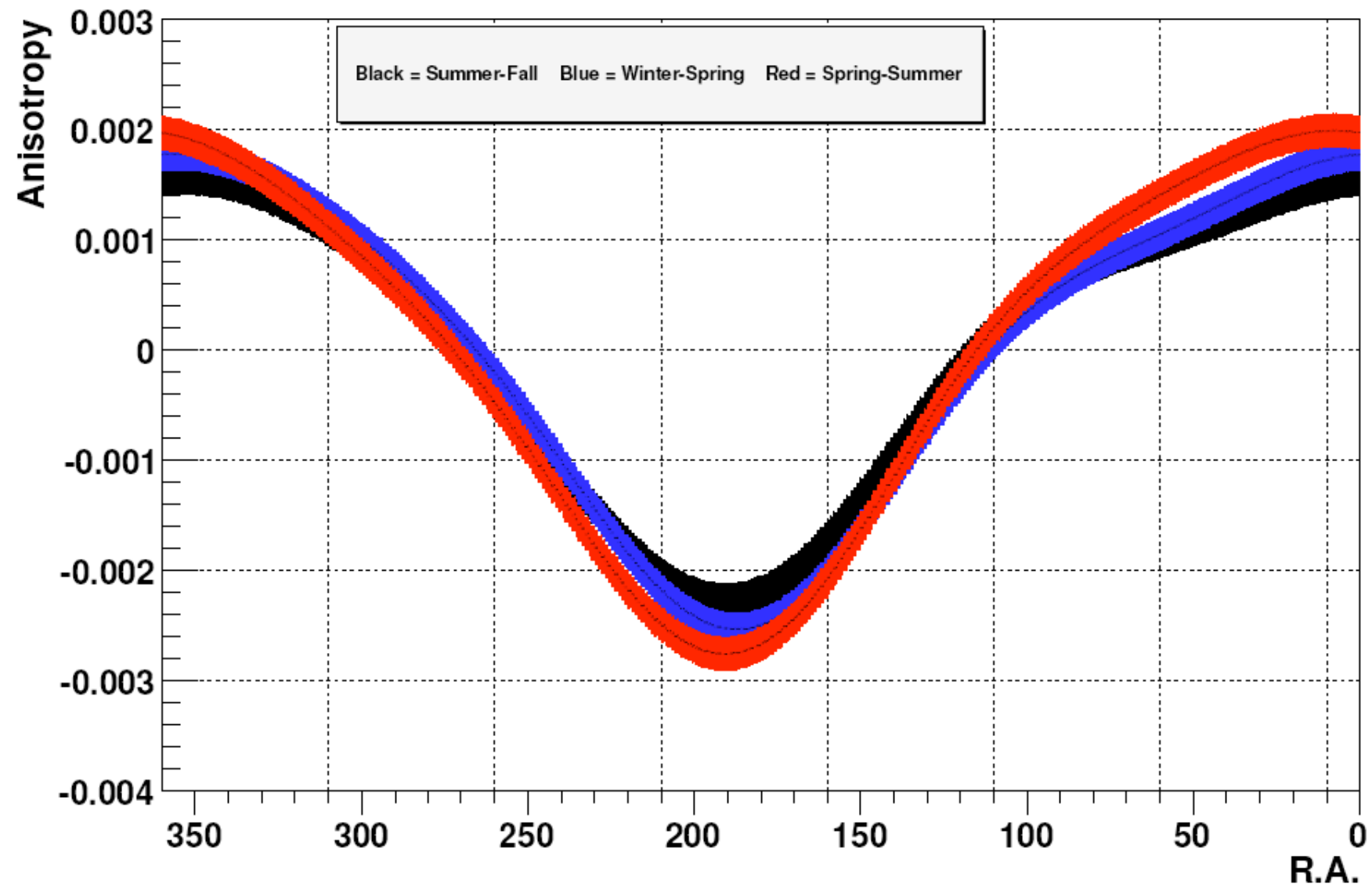


Sky Map of CR large scale anisotropy

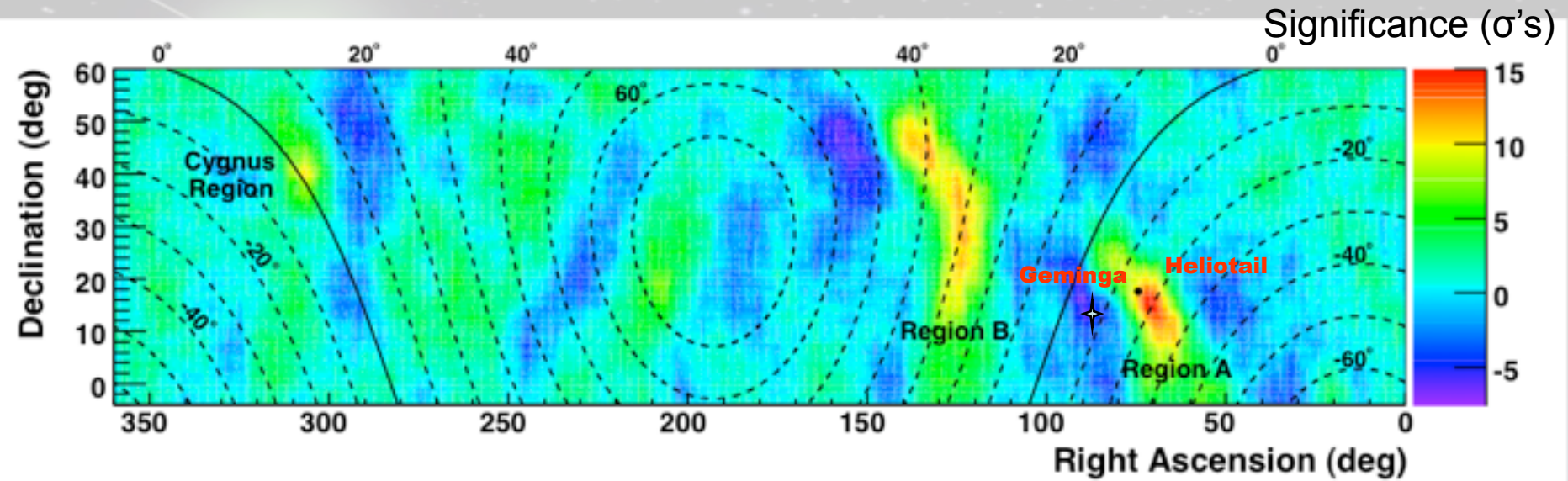
Similar results to Tibet and Super-K (and now IceCube)



Seasonal Variation

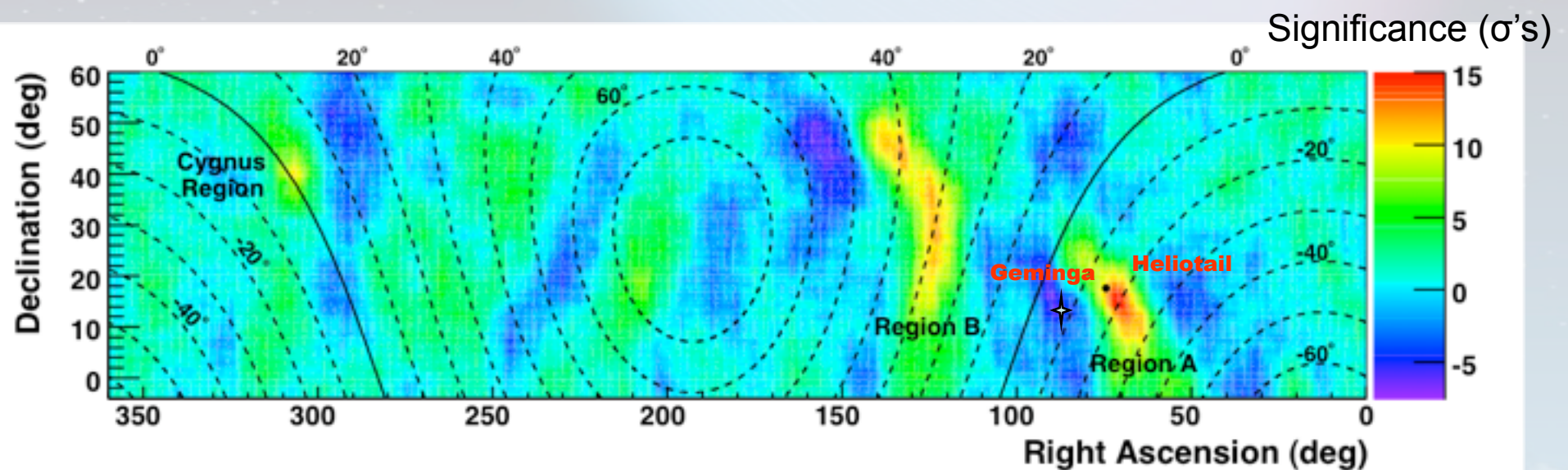


Cosmic Ray Observations

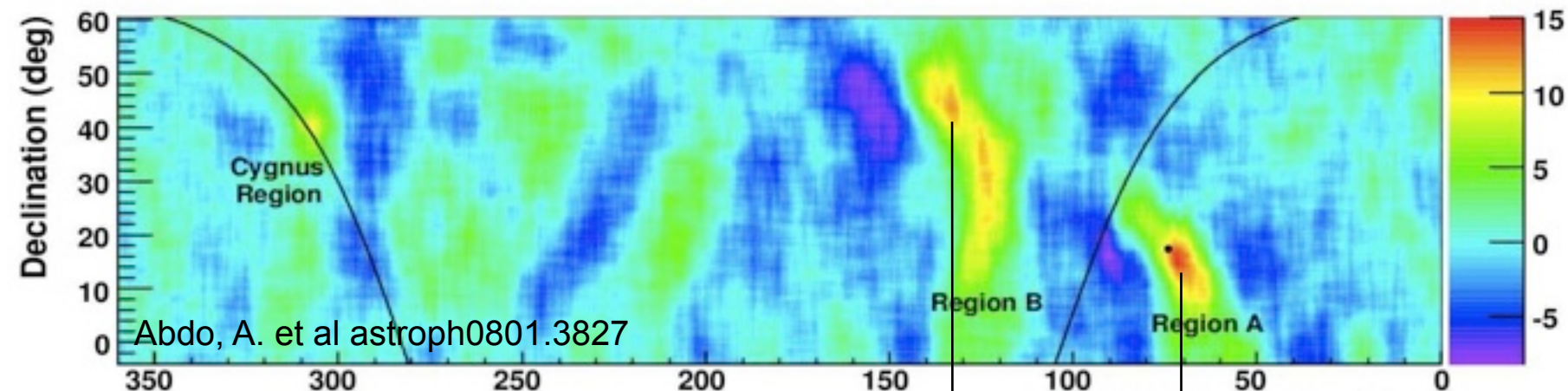


- No weighting or cutting.
- Map dominated by *charged* cosmic rays.
- 10° smoothing, looking for intermediate sized features.
- Two regions of excess 15.0σ and 12.7σ . Fractional excess of 6×10^{-4} (4×10^{-4}) for region A(B).

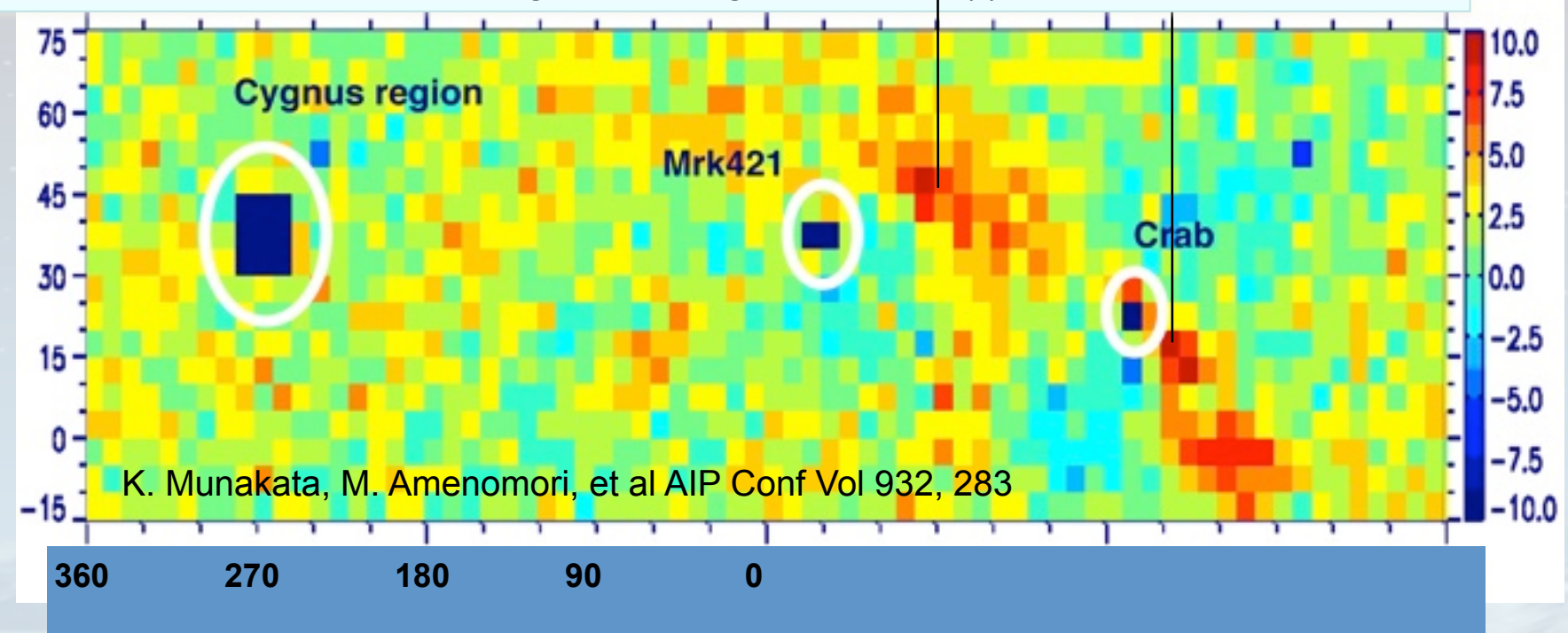
- Anisotropy on the 5-10 degree scale.
- Peak excess $\sim 7 \times 10^{-4}$ (much smaller than the LSA)
- Explanations are difficult because the gyro-radius of a 10 TeV proton in a 1 μG field is 0.01 parsecs=2000 AU



Milagro Observation using Background Calculation over 2 hour (30° in RA) intervals

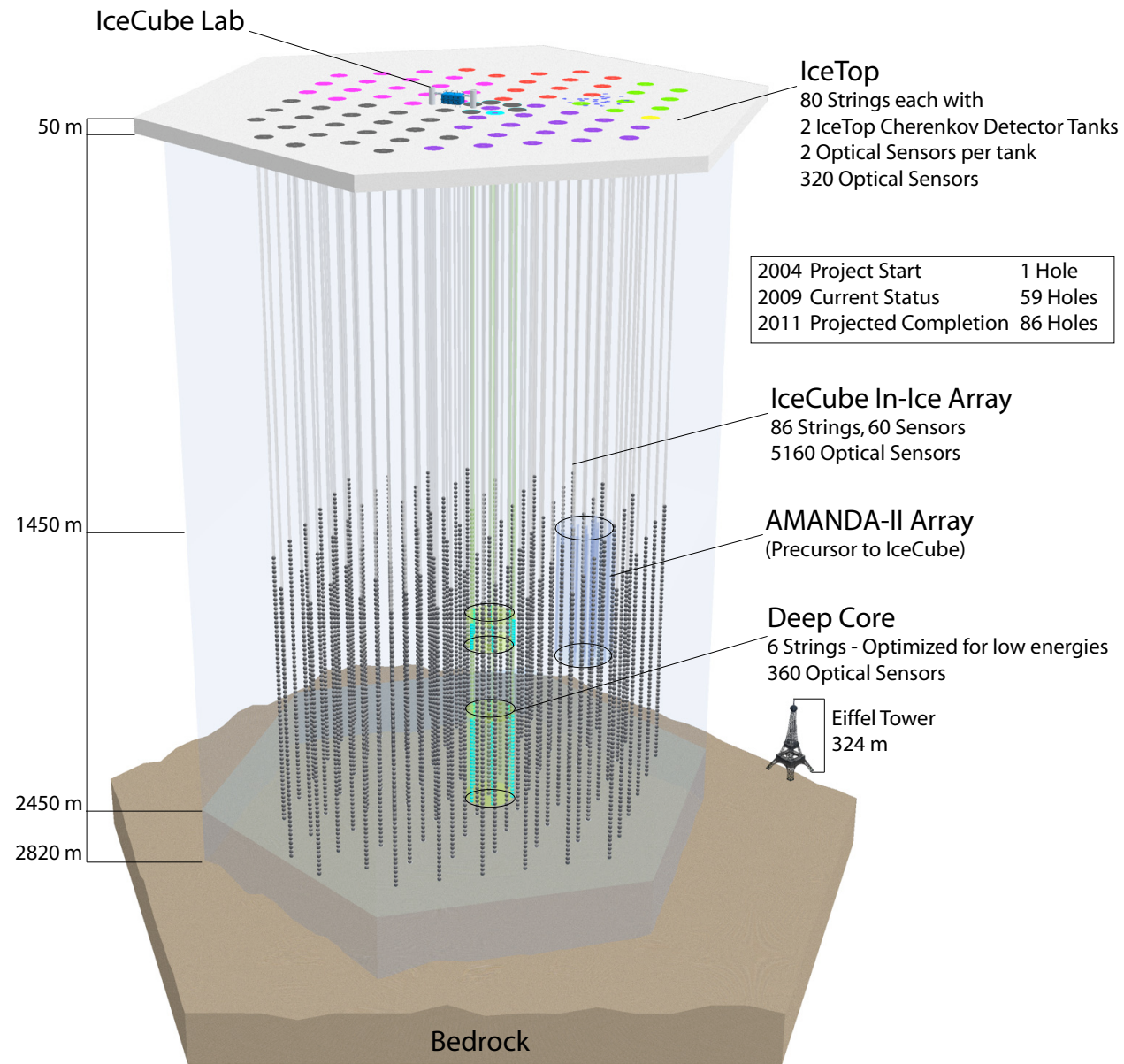


Tibet AS Observation after subtracting model of large scale anisotropy



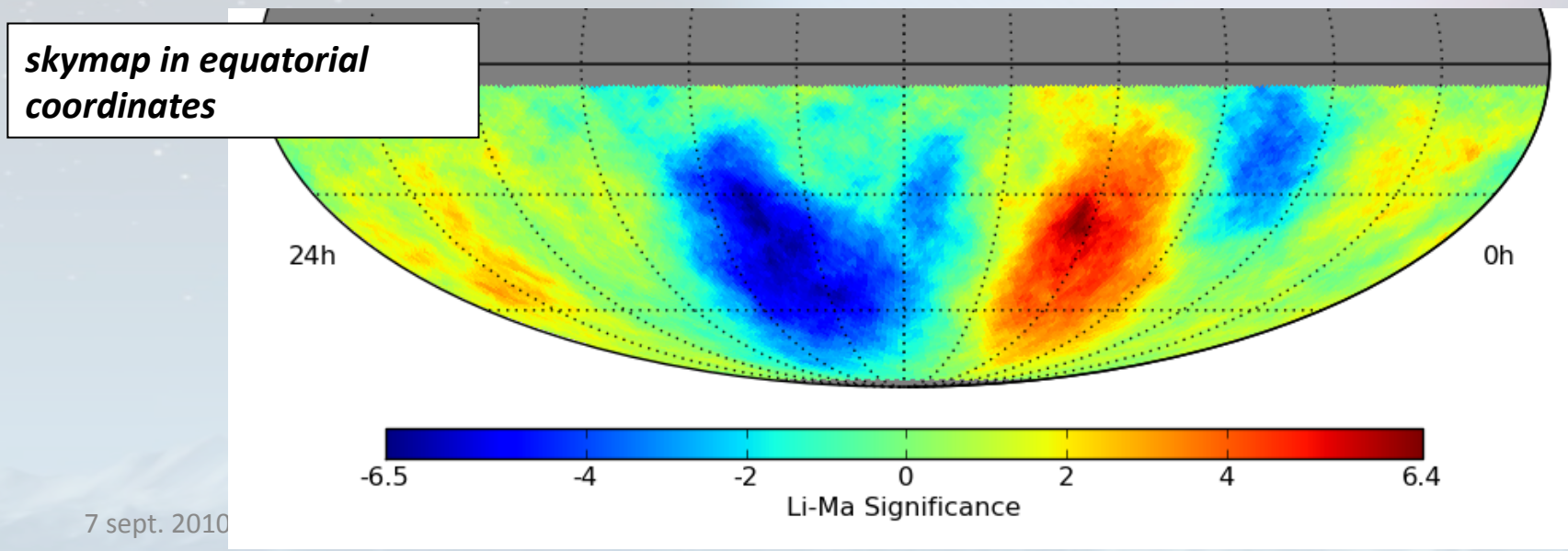
K. Munakata, M. Amenomori, et al AIP Conf Vol 932, 283

IceCube

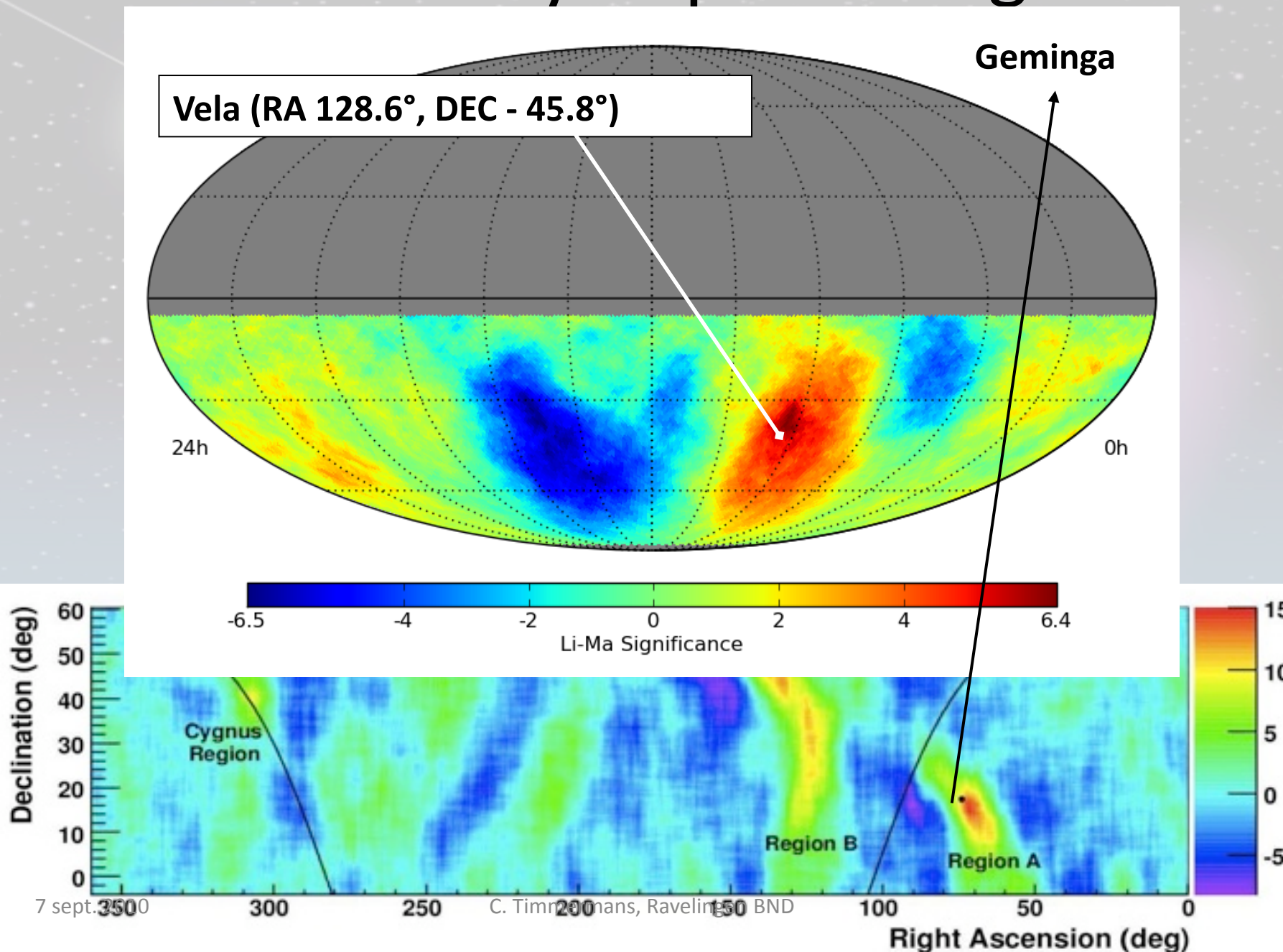


IceCube maps Galactic cosmic rays

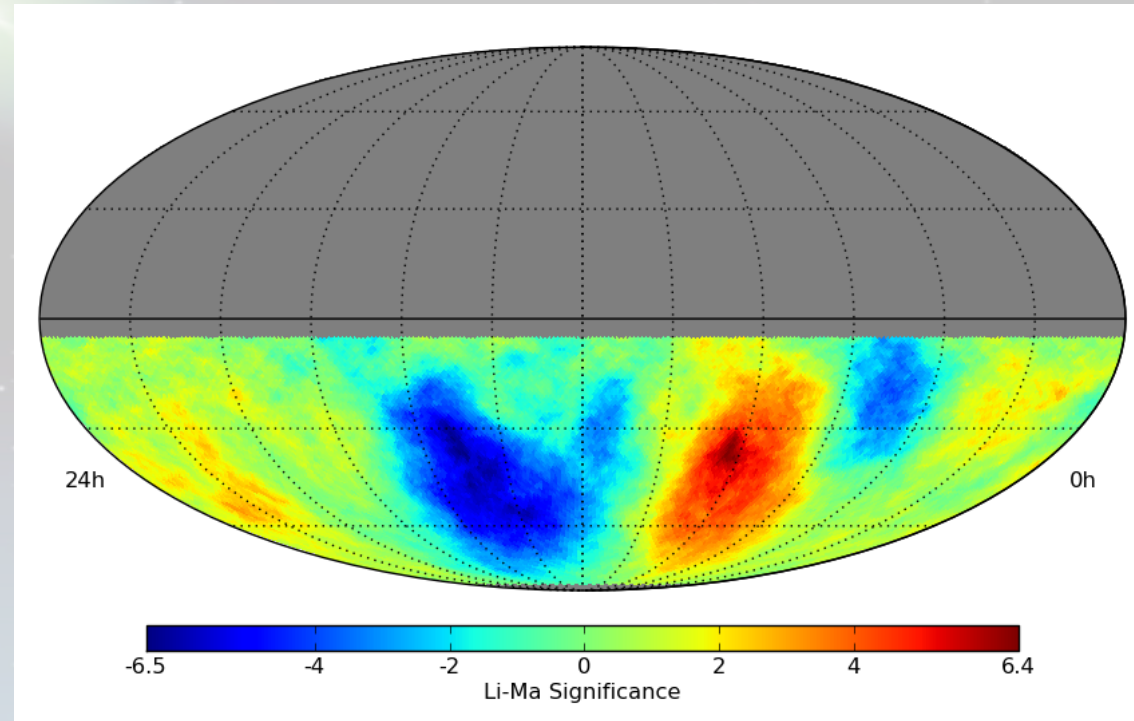
- By measuring downward going muons from air showers, IceCube can study the arrival direction distribution of cosmic rays in the energy range \sim 10 TeV to several 100 TeV and *produce a cosmic ray sky map of the southern sky*.
- The arrival direction distribution *is not isotropic*.
- At these energies, cosmic rays are Galactic, and by studying these anisotropies, we can hope to learn about the *origin of Galactic cosmic rays*.



IceCube 40 skymap vs Milagro



Conclusions CR below the knee



- first view of cosmic ray sources in... muons ?
- new structure in the Galactic magnetic field ?
- Geminga in northern hemisphere (Milagro,...)